Sustainable Engineering Internship 2022

Final Report

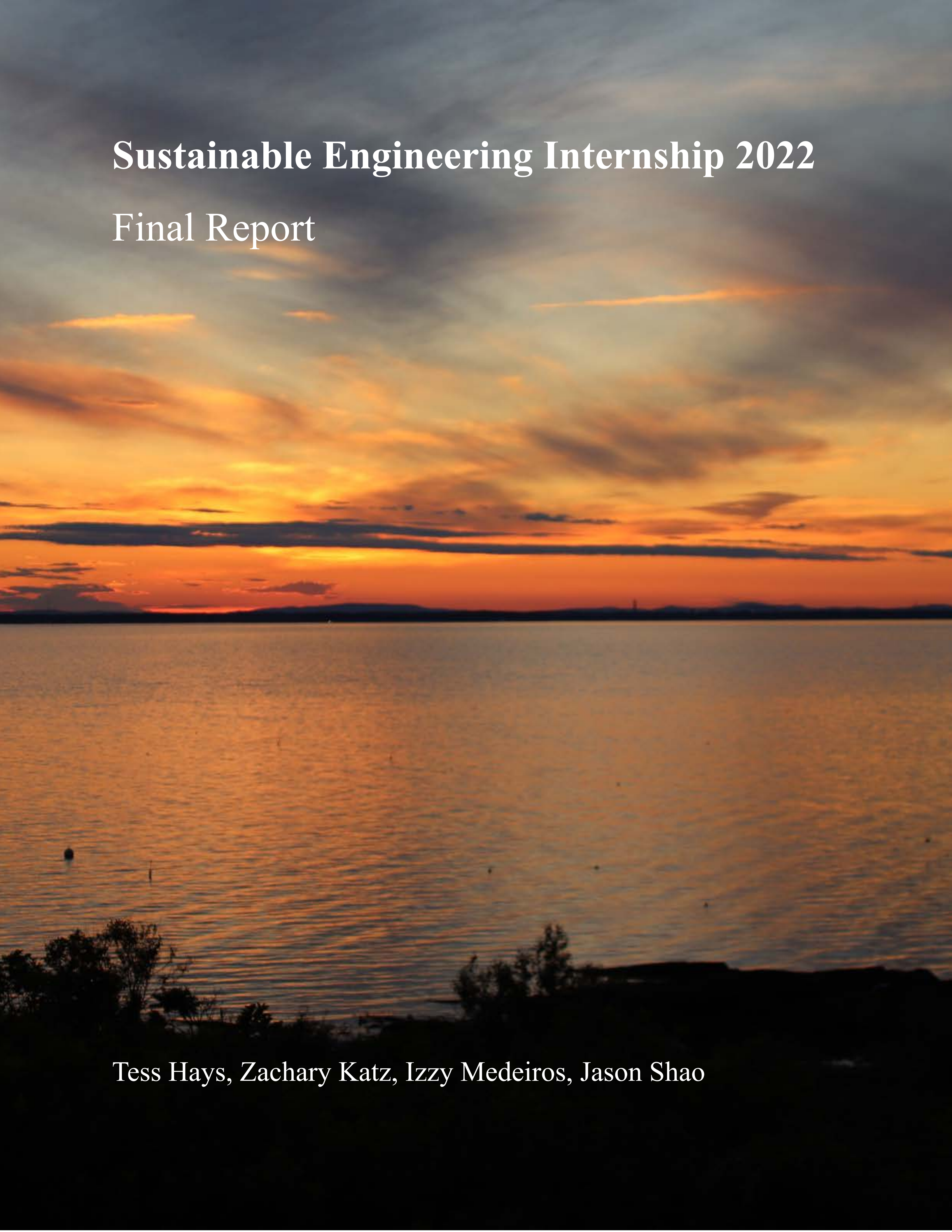

Tess Hays, Zachary Katz, Izzy Medeiros, Jason Shao

Table of Contents

List of Figures

List of Tables

1 Tilting a Windmill

Lead Interns: Zachary Katz, Izzy Medeiros

1.1 Background

SML has a Bergey wind turbine on a custom made 80’ monopole tower that uses a hydraulic cylinder and a counterweight to raise and lower the turbine. This occurs during seasonal blade installation and removal, in addition to when maintenance is needed. When the turbine is lowered, hydraulic fluid overflows the reservoir; when the tower is raised, this excess fluid must be added back into the system to properly extend the cylinder. Thus, every time the tower is raised or lowered, multiple staff members are required to add extra hydraulic fluid or catch overflowing hydraulic fluid.

1.2 Purpose and Scope

SML tasked the interns with designing an upgrade to the existing hydraulic system of the turbine. With this upgrade, the necessary amount of fluid for lowering and raising the turbine would already be in the system, so there would be no running out or fluid overflow. This would also eliminate the need for multiple staff members to catch excess fluid. The interns must determine the amount of hydraulic fluid necessary and reservoir size needed to achieve this goal, then determine how the proper size reservoir can be incorporated into the existing system. They will gain a working knowledge of how the hydraulic system functions on the tower, identify all the working parts, calculate how much fluid is needed in the system, and calculate how big of a reservoir is needed to retain all the fluid and not overflow or run out when performing its intended function. They will provide some design drawings with dimensions that fit the existing set-up.

1.3 Methods

General hydraulic systems were researched and the existing hydraulic system was analyzed to understand how it works. A simple hydraulic system, like the one installed on the turbine, typically consists of a fluid reservoir, pump, hydraulic cylinder, piping, and hydraulic fluid. As the system is operated, hydraulic fluid is pumped through the pipes from the reservoir to the bottom of the hydraulic cylinder, extending the cylinder. The cylinder on the turbine has a connection at both ends, so it is considered double-acting. When the cylinder is to be retracted, hydraulic fluid is pumped into the top of the cylinder (Figure 1.1). Where fluid is pumped is controlled by a switch and monitored by a pressure gauge.

Figure 1.2 shows an overview of the hydraulic system of the wind turbine, showcasing the same parts in Figure 1.1 on the real system.

The current hydraulic tank was measured to be 15” x 10” x 5” on the outside, for a maximum interior volume of 900 cubic inches, Equation 1.1 (Figure 1.3).

$$V_{tank} = 15in * 10in * 6in = 900in^3 \approx 3.9\ gallons \tag{1.1}$$

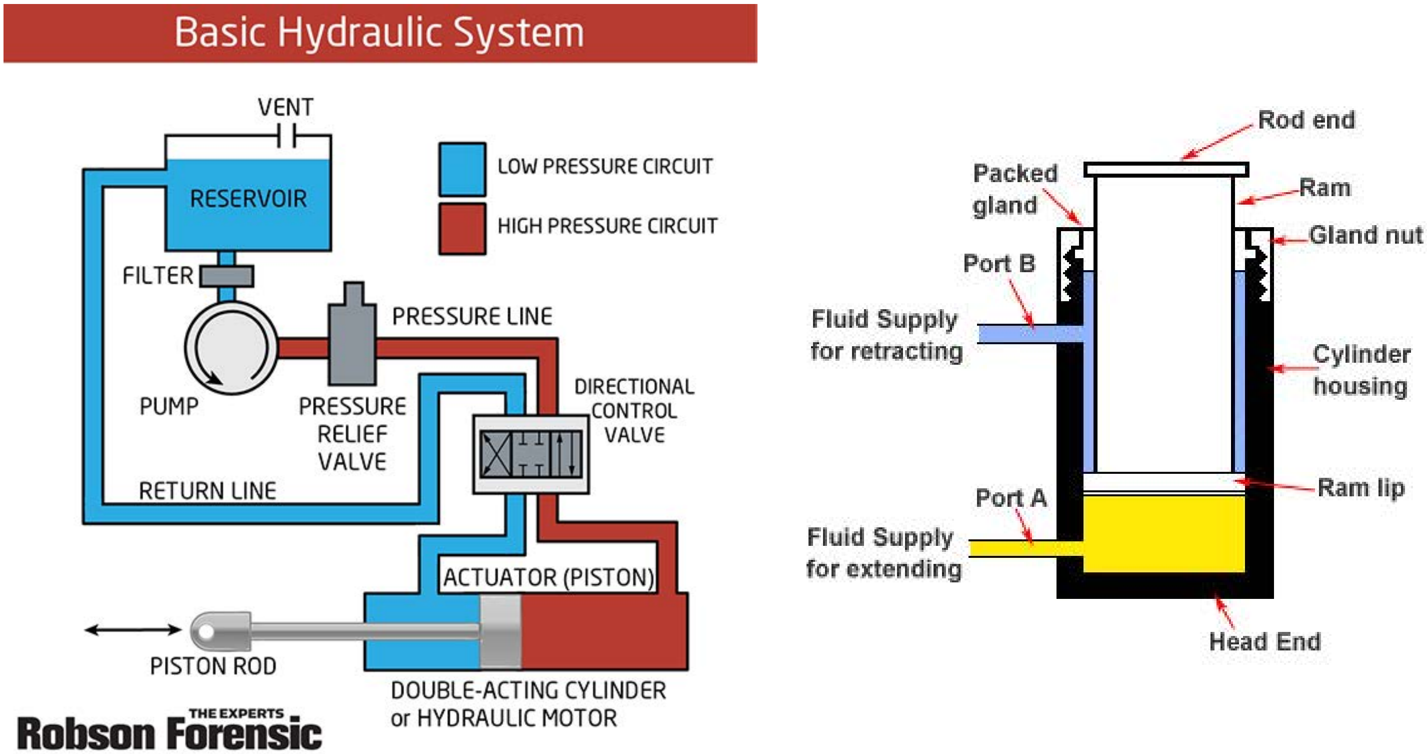

Figure 1.1: Left: A simple hydraulic system. Fluid is pumped from the reservoir through the directional control valve to the bottom of the double-acting cylinder via the high pressure circuit, extending the cylinder. When the cylinder is to be retracted, the directional control valve allows the high pressure fluid to enter by the top of the cylinder, pushing the cylinder back down.
Right: Double-acting hydraulic cylinder principle. When the cylinder is to be extended, fluid flows into port A, pushing the cylinder up; when the cylinder is to be retracted, fluid flows into port B, pushing the cylinder down and pushing the fluid in port A into the reservoir.

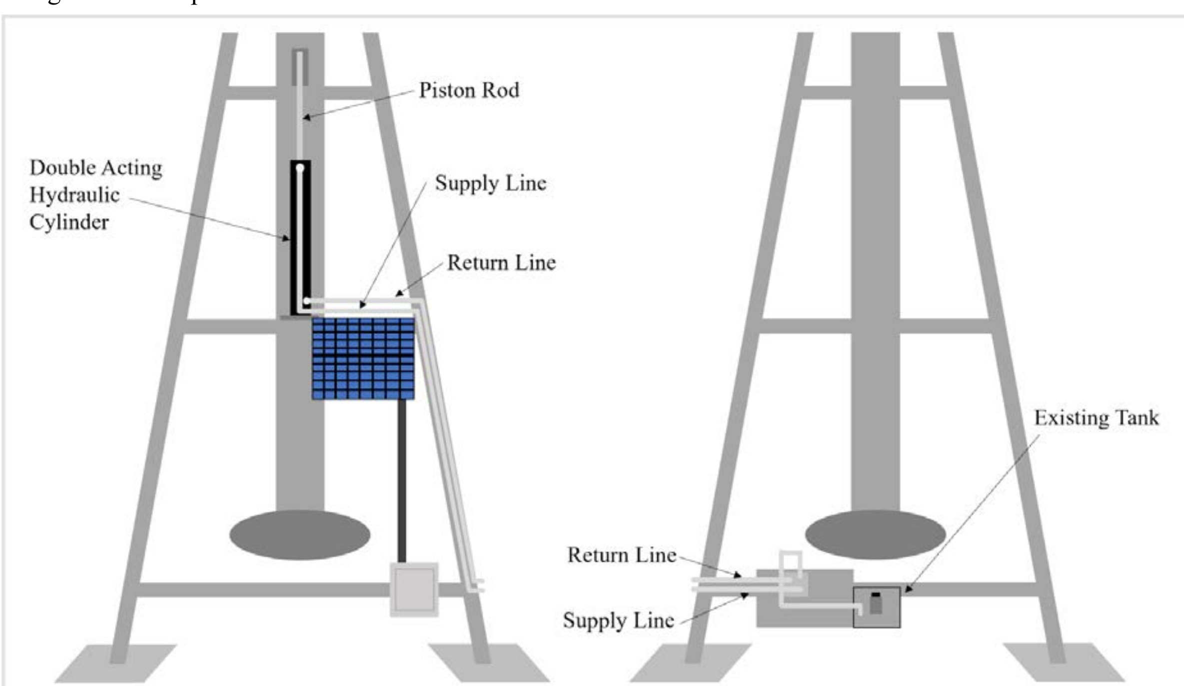

Figure 1.2: Overview photo of the wind turbine hydraulic systems showing the similarity of the system to Figure 1.1.

Figure 1.3: Hydraulic reservoir tank. The right side is a separate sheet of metal bolted to the rest of the tank and fitted with a gasket.

From manufacturer's specifications, the hydraulic cylinder has a 5" bore and 60" stroke, for an interior volume given as 1180 cubic inches by the formula for a cylinder, Equation 1.2 (Figure 1.4).

$$V_{cylinder} = \pi r^2 l = \pi (2.5in)^2 * 60in = 1180in^3 \approx 5.1\ gallons \tag{1.2}$$

NORTHERN HYDRAULICS

Welded Cross Tube Cylinder - 5" Bore

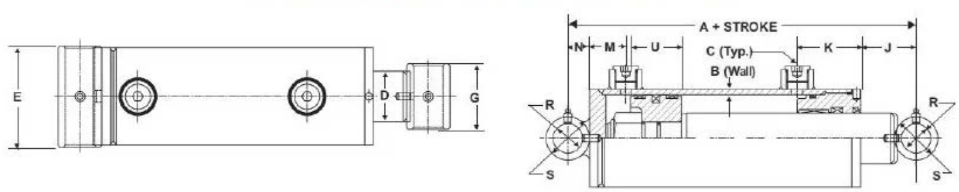

Dimensional Data in Inches (Millimeters)

BORE	A*	B	C	D	E	G	J	K	M	N	R	S	T	U
5.000 (127)	11.00 (279.4)	0.250 (6.4)	3/4" NPT	2.500 (63.5)	5.750 (146.1)	4.000 (101.6)	2.750 (69.9)	3.000 (76.2)	2.000 (50.8)	1.250 (31.8)	1.515 (38.5)	2.500 (63.5)	6.250 (158.8)	2.00 (50.8)

*Dimension * A 2.000 (50.8) spacer is added at 48.000 (1219.2) stroke, and an additional 1.000 (25.4) is added for each additional 6.000 (152.4) of stroke thereafter to a 6.000 (152.4) Maximum spacer. ** For 2.0" with 1.0" pins "J" = 2.32", For 2.5" with 1.0" pins "J" = 3.00". ***For 2.0" and 2.5" bore there are additional cylinders the difference being R = 1.015" and S = 1.500". (25.8) Note: 5", 6" and 8" bores have an externally mounted retainer ring.

Figure 1.4: Hydraulic cylinder specification sheet showing the 5" bore, 60" stroke, and hydraulic fluid inputs into the cylinder.

The interns estimated the length of pipe to be 40 feet and measured the circumference as 2.5 inches. The formula for a cylinder, Equation 1.3, was used to determine the volume as 188 cubic inches. This is likely an overestimate due to the thickness of the pipe itself, which will help ensure the proposed system is adequately sized.

$$V_{pipe} = \pi r^2 l = \pi(0.4in)^2 * 20ft = 241in^3 \approx 1\ gallon \tag{1.3}$$

Measurements were converted to gallons and compared to the plans provided for the system (Figure 1.5). These plans specifically show how to arrange hoses to flush out the system, but the general flow of hydraulic fluid (labeled as oil) can be seen. The tank is listed as 3.5 gallons, compared to the measured 3.9 gallons. This discrepancy may be due to the thickness of tank walls (the outside of the tank was what was measured) and/or baffles in the tank. The pipes are listed as 0.375 gallons, compared to the measured 1 gallon, and the cylinder cavity is listed as 2.5 gallons, compared to the measured 5.1 gallons. These discrepancies are not easily explained by differences in interior versus exterior diameter.

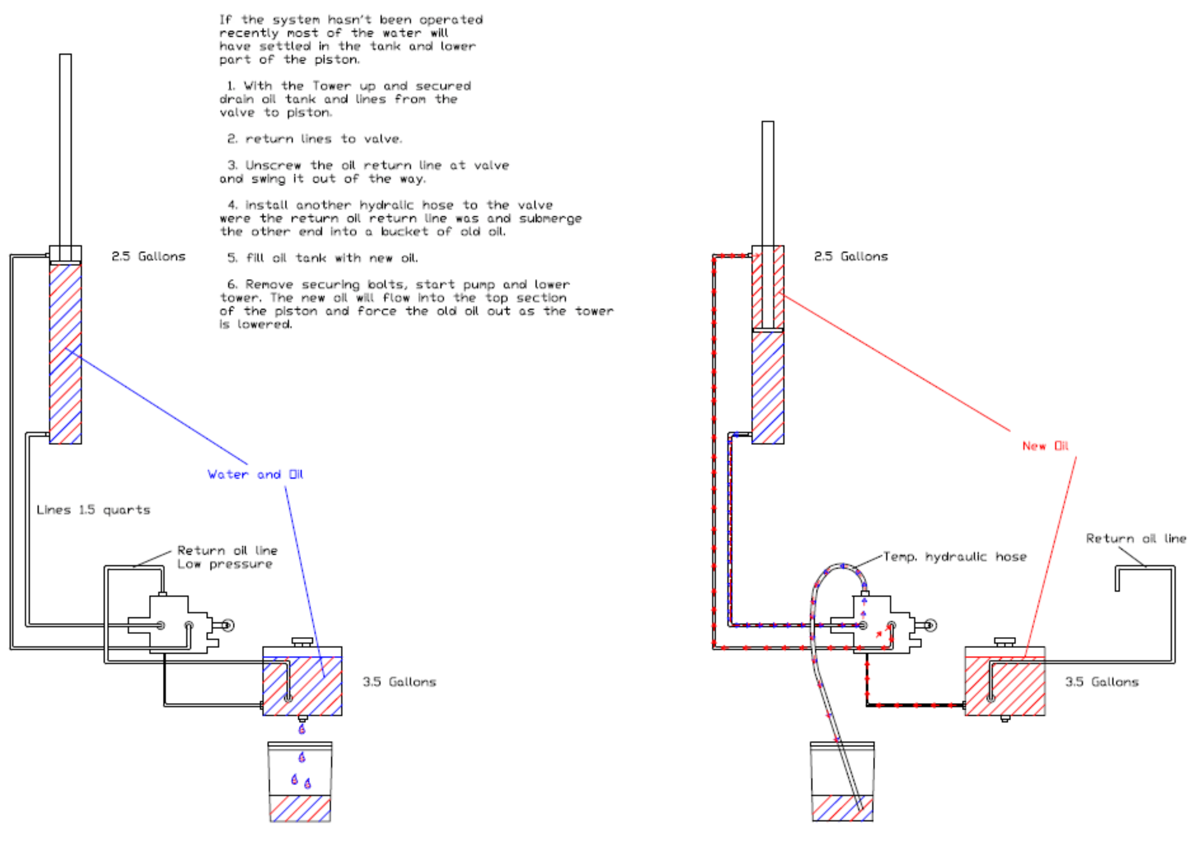

Figure 1.5: Original schematic of the wind turbine hydraulic system showcasing fluid pipelines and how to change out the hydraulic fluid. The interns recalculated the volume measurements given, showing that the current reservoir is inadequately sized for the amount of hydraulic fluid needed to extend the cylinder.

When the cylinder is extended, a minimum of 5.1 + 1 = 6.1 gallons of hydraulic fluid is needed. However, when the cylinder is retracted, most of the hydraulic fluid drains to the tank, which is only 3.9 gallons. This matches Ross' description of needing to add more fluid when the cylinder is being extended and a few gallons of overflow when the cylinder is retracted. An excess of at least 6.1 - 3.9 = 2.2 gallons of fluid overflows each cycle, with the true amount likely greater due to thermal expansion and/or aeration of the hydraulic fluid.

1.4 Design and Analysis

It is recommended to design a hydraulic fluid reservoir with at least 20% excess space for thermal expansion and aeration of the hydraulic fluid during operation (Fundamentals of Hydraulic Reservoirs). In addition, the length and cross-sectional area of the pipes were estimated from external measurements, so the excess space accounts for underestimates. The interns recommend a more conservative total reservoir volume of 1620 cubic inches or 7.3 gallons. This allows for a 20% tolerance over the 6.1 gallons needed for cylinder operation for thermal expansion, aeration, and estimations in calculations.

A hydraulic system reservoir is not just designed to store fluid; in addition, it must allow heat transfer to the environment, space for fluid to slow down and contaminants to settle, and access to remove and add fluid (Fundamentals of Hydraulic Reservoirs). With these design criteria in place, several tank options were considered.

The far wall of the existing tank is made of a separate sheet of metal and bolted to the rest of the tank, allowing for easy removal. When removed, a new tank can be constructed with a flange that can be easily bolted to the same ring of metal the far wall was attached to. The simplest design involves adding a 24" x 8" x 4" tank to the right side of the existing tank, for an additional volume of approximately 3.33 gallons and total volume of 7.23 gallons (Figure 1.6). This design lifts the base of the additional tank above the existing tank's base, helping promote fluid flow towards the outlet pipe.

Another possibility is to connect a tank by the drain of the first tank (Figure 1.7). This method utilizes a u-shaped connection to allow the tanks to fill evenly. However, with this option, both the input and output valves would be in the first tank, with the u-pipe hindering fluid flow and mixing between the tanks while in operation. This design utilizes a 13" x 10" x 6" tank, for an additional volume of approximately 3.38 gallons and total volume of 7.28 gallons.

Each of these options add between 3.3 and 3.4 gallons of storage to the existing tank, providing the necessary space and tolerance for the hydraulic cylinder to be operated without fluid overflow or needing to add excess fluid.

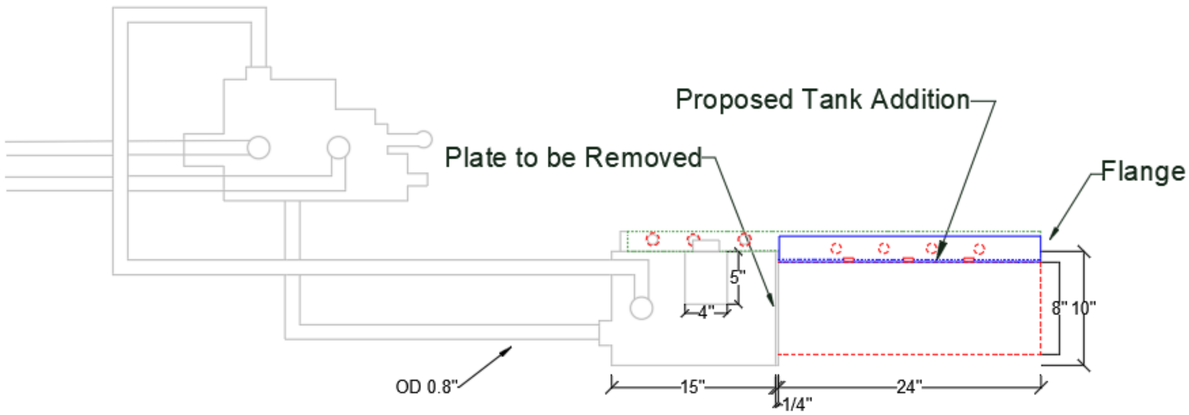

Figure 1.6: CAD drawing of proposed hydraulic reservoir via removal of side plate and addition of 8” x 24” x 4” tank with flanged side to fit against existing tank. An additional flange is added on top to support the weight of the new tank.

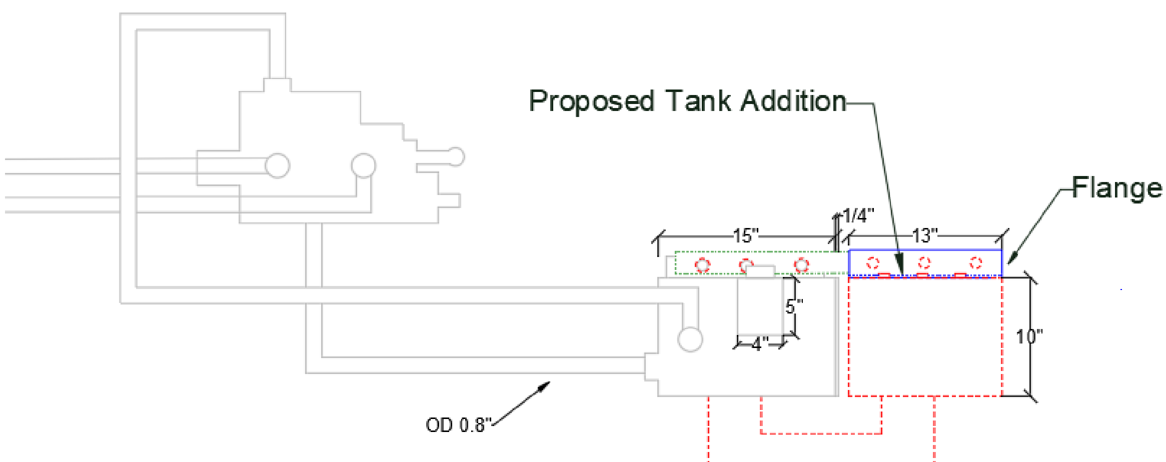

Figure 1.7: CAD drawing of proposed hydraulic reservoir via addition of a 10” x 13” x 6” tank and u-shaped connection to the existing tank. A flange is added on top to support the weight of the new tank.

1.5 Conclusions and Recommendations

Although both tank addition options presented are reasonable, the interns recommend the attached square tank because of its simplicity. Because the system is typically only used twice a year, time for fluid to slow down and contaminants to settle is not a major concern, even if both the inlet and outlet are on the same side of the tank. Furthermore, the lower elevation of the outlet compared to the tank extension will naturally allow fluid to flow towards the outlet. The attached square tank will also be easier to remove if cleaning of the reservoir is necessary.

It is also recommended that the amount of fluid leaking as the cylinder is compressed be measured to ensure the volume of the tank suggested is reasonable before installing a larger tank.

1.6 References

Fundamentals of Hydraulic Reservoirs, Power and Motion, 1 January 2012

Green, John, *Failures & Fundamentals: Hydraulic Systems*, Robson Forensic

Harikesh, Divedi, *Working Principle of Double Acting Hydraulic Cylinder*

Khayal, Osama, *Introduction to Hydraulic Systems*, July 2017

Northern Hydraulics, *5" Bore X 60" Stroke Welded Cross Tube Mount Cylinder, 3000 PSI,* https://northernhydraulics.net/catalog/5-bore-welded-cross-tube-3500-psi/5-bore-x-60-stroke-welded-cross-tube-mount-cylinder-3000-psi-2049.html

Learning and Knowledge Development Facility, *Basic Level Mechanics 3: Hydraulics*, United Nations Industrial Development Organization

2 The Power of Wind

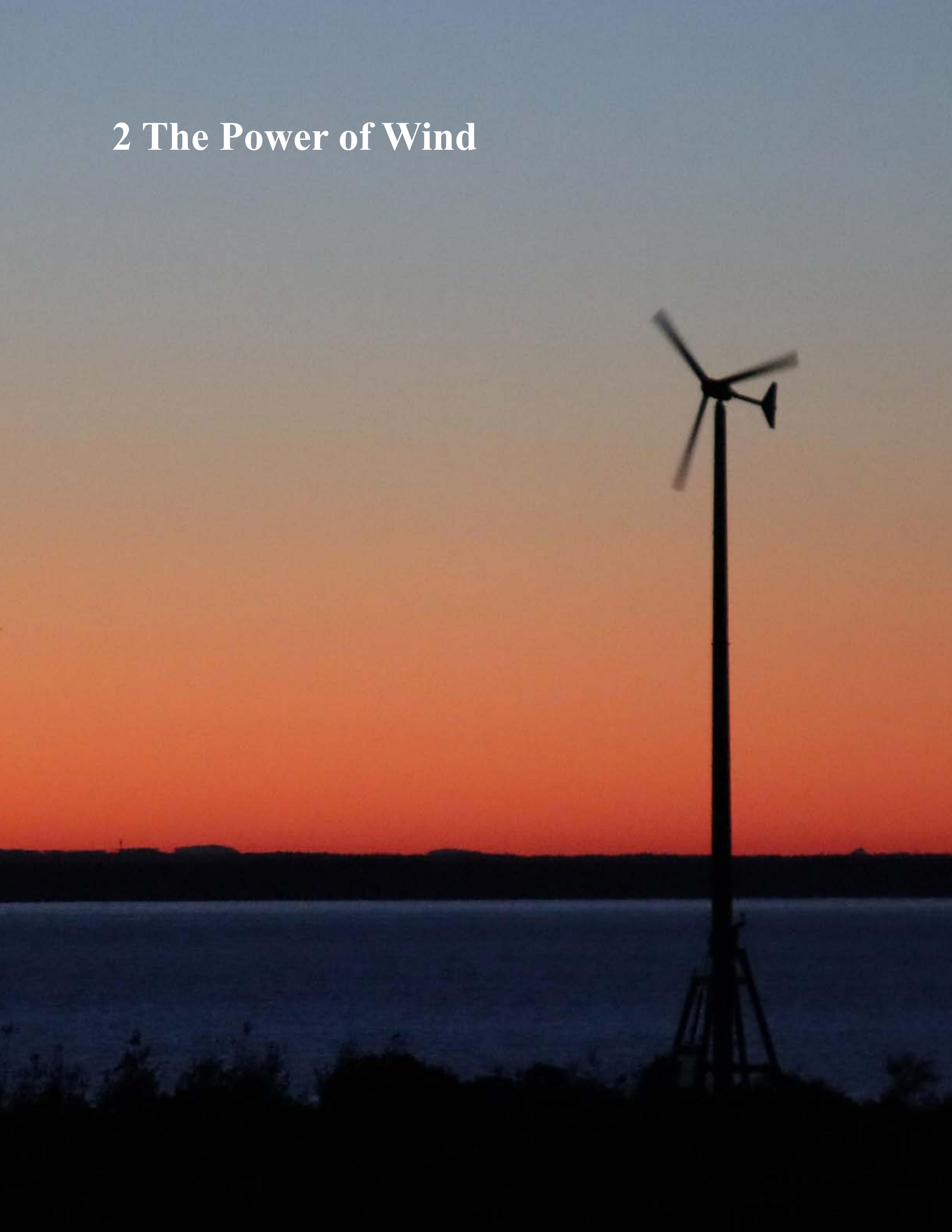

Lead Interns: Zachary Katz, Jason Shao

2.1 Background

Shoals Marine Laboratory (SML) operated a 7.5kW Bergey wind turbine from 2007 until the spring of 2019 when the turbine experienced an internal electrical failure. The unit was replaced on June 18th 2021 with a 10kW version and an upgraded charge controller (Elzweig et al., 2021). Wind power contributes significantly to SML's green energy grid because it has the capability of providing power at night and during stormy weather when the island's photovoltaic systems are less effective. The wind energy data is displayed on SML's dashboard (https://sustainablesml.org/) with the use of an Accuenergy AcuDC power meter.

The 2021 Sustainability Engineering Interns started an analysis to quantify the power output of the turbine compared to the theoretical power in the wind. They reported an average power coefficient (Cp) of 0.21, given by Equation 1,

$$C_p = \frac{P_{measured}}{P_{theoretical}} = \frac{P_{measured}}{\frac{1}{2}\rho A U^3} \tag{2.1}$$

where rho is the density of air (assumed 1.225 kg/m^3), A is the area swept out by the turbine blades, and U is the wind speed at the turbine height.

Currently, there are two instruments providing readings of instantaneous power output for the wind turbine, the Bergey charge controller (VSCII) and the AcuDC. However, readings from these devices currently provide different values for the instantaneous power output. The 2021 interns corrected for the readings by plotting several instantaneous comparisons between the outputs of the two meters and calculating a line of best fit, but also suggested recalculating using more data. To adjust for the offset there is currently a -.29 kW correction applied to the AcuDC data before it is displayed on the Dashboard.

2.2 Purpose and Scope

Shoals wants to understand how their wind turbine investment compares to the rated specifications. Additionally, they aim to display accurate and reliable data on their dashboard. The interns were tasked with monitoring the meters to determine where the discrepancies between each meter are coming from, and comparing these data to theoretical power outputs based on wind speed. After this, interns should be able to make a recommendation on how to better adjust for the discrepancy on the dashboard.

2.3 Methods and Results

2.3.1 Wind Speed at Hub Height

There are two nearby anemometers, one on top of the Appledore Island Radar Tower at 43 meters above mean sea level (AMSL) and one on White Island at 32.3 meters AMSL. To measure the Radar Tower anemometer height, first the base elevation of the tower was estimated as 67 feet using the 4th edition 2015 SML topographic map by W. E. Bemis. (Appendix A). Then, the distance to the roof of the tower was measured to be 19.32 meters using a surveying tape measure. Finally, the height of the anemometer above the tower roof was measured as 127 inches. Combining, the approximate height of the Radar Tower anemometer is 43 meters AMSL. This measurement differs from the previously used value of 54 meters which was obtained from a GPS at the top of the tower. The error of a GPS' vertical measurements is considerably greater than horizontal measurements because of the configuration of satellites. Therefore, the interns believe that the 43 meter measurement is more accurate. The distance from the anemometer to the first narrowing of the tower near the bottom was measured as 21.29 meters, which may be useful in future studies if a more accurate height is desired (Figure 2.1). The White Island anemometer height is provided by NOAA, and the turbine height is as given on the dashboard (National Data Buoy Center).

The yawing turbine makes placement of an anemometer at the turbine hub difficult. Thus, the wind data from either the Radar Tower or White Island must be corrected to obtain a wind speed estimate to use in the power calculation. There are two common ways of correcting for height in wind speed, a power law,

$$U(z) = U(z_r)\left(\frac{z}{z_r}\right)^{\alpha} \tag{2.2}$$

or a log law,

$$U(z) = U(z_r)\ln\frac{\left(\frac{z}{z_0}\right)}{\left(\frac{z_r}{z_0}\right)} \tag{2.3}$$

Figure 2.1: Ledge of Radar tower as measured for future studies, even with top of exterior stairs and base of door.

where U(z) is the wind speed at a desired height z, U(z_r) is the known wind speed at a reference height z_r, α is a parameter commonly about 1/7, and z_0 is the roughness scale length, qualitatively chosen based on the Davenport-Wieringa roughness classification, Figure 2.2 (Wosnik, M., 2019).

Terrain description	z_0 (mm)
Very smooth, ice or mud	0.01
Calm open sea	0.20
Blown sea	0.50
Snow surface	3.00
Lawn grass	8.00
Rough pasture	10.00
Fallow field	30.00
Crops	50.00
Few trees	100.00
Many trees, hedges, few buildings	250.00
Forest and woodlands	500.00
Suburbs	1500.00
Centers of cities with tall buildings	3000.00

Figure 2.2: Surface roughness length z_0 scale.

The log law is typically accurate from 0-100 meters above the surface, while the power law is typically accurate starting 20 meters above the surface (Wosnik, M., 2019). The turbine hub height is 36.4 meters AMSL, so both laws were tested to find the best agreement between the White Island and Radar Tower anemometers. SML's Dashboard displays a graph of the wind speed data from both anemometers in addition to the power recorded on the AcuDC, with a minutely CSV file also including wind direction available for download (Figure 2.3). For this study, data from June 19th 2021 until June 23rd 2022 was utilized.

Because the White Island anemometer is below the turbine hub height and wind speed typically increases with height, correction factors of either law will increase wind speed. Because the Radar Tower anemometer is above hub height, correction factors of either law will decrease wind speed. However, as the White Island wind speed is typically greater than the Radar Tower measurements (Figure 2.3), any attempted correction will necessarily increase the discrepancy between measurements. It is expected that these nearby stations, when corrected to a common height, produce similar wind speeds. However, discrepancies occur and are likely due to complex island topography.

Several values of α near 1/7 were tested in the power law and several values of z_0 were tested in the log law with data ranging from 19 June 2021 until 23 June 2022 (Appendix B). As expected, lower values of each variable produced a better fit. The interns chose the power law with an alpha of 0.1, which produced the smallest discrepancy in wind speed at turbine height using data from White Island versus the Radar Tower while still maintaining a reasonable increase of wind speed with height. A histogram of corrected wind speed for both White Island and the Radar Tower was plotted, and these were fit with a Rayleigh distribution (Figure 2.4). For the α=0.1 power law, the mean corrected wind speed from the White Island anemometer was 6.55 m/s and the mean corrected wind speed from the Radar Tower anemometer was 6.25 m/s.

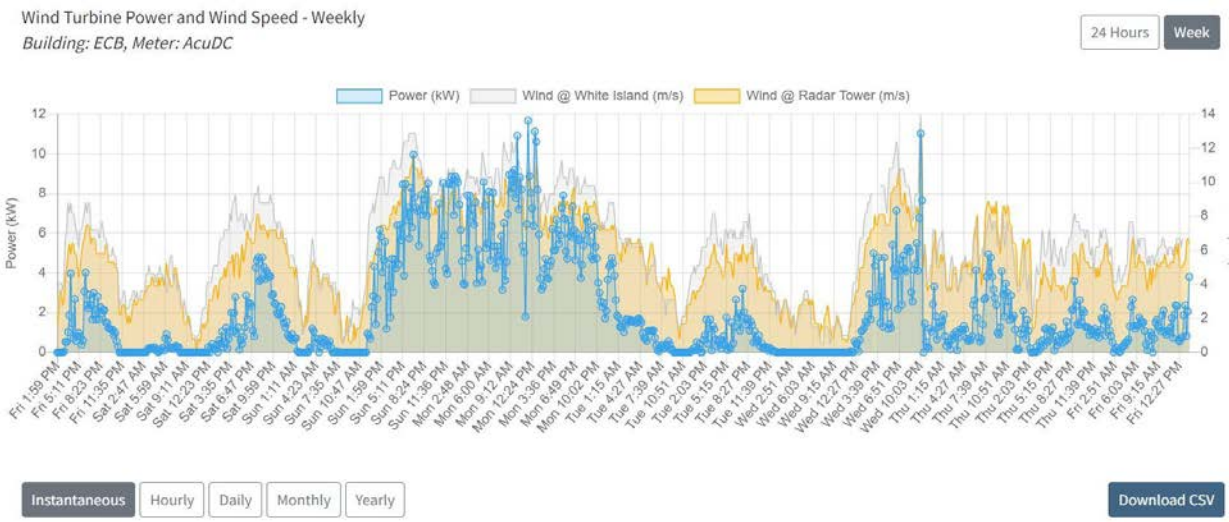

Figure 2.3: Example Shoals dashboard wind data for Friday June 24th 2022 through Friday July 1st 2022. The White Island wind speed, in white, is generally faster than the Radar Tower wind speed, in orange. The power output is also shown.

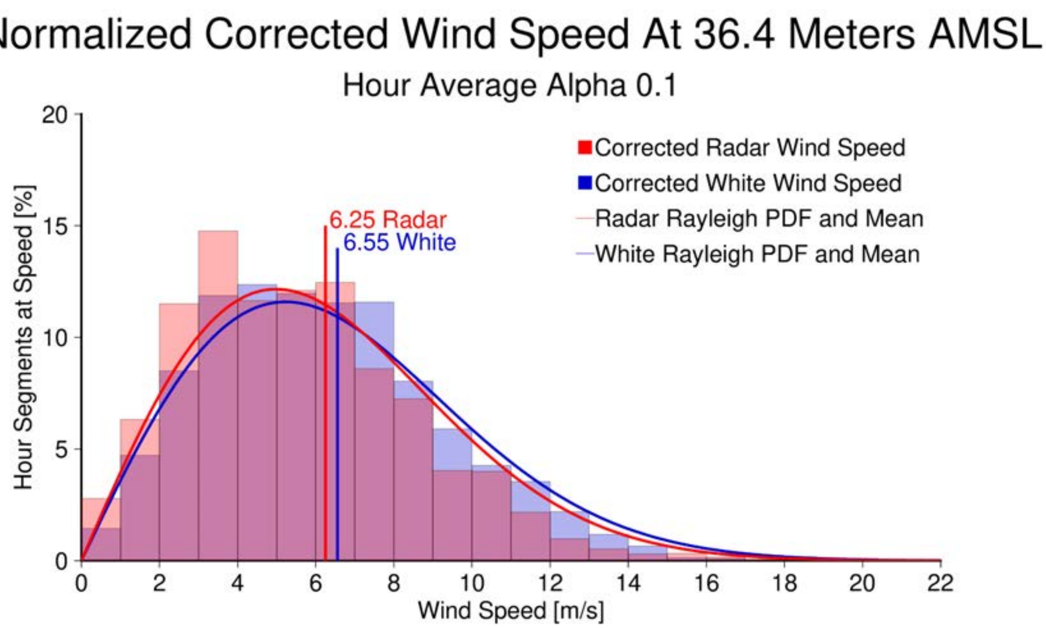

Figure 2.4 Alpha = 0.1 corrected wind speeds normalized histogram for June 19 2021 - June 23 2022 of both White Island and Radar Tower anemometer readings, with a fitted Rayleigh probability density function (PDF).

Next, a time series of wind speed adjusted to hub height was determined. Again, the consistent faster wind speeds at White Island are observed, and no long-term anomalies were found. There is strong correlation between the White Island and Radar Tower recordings, as evidenced by an example plot of 10 minute averages selected to include a range of wind speeds spanning May 15th - May 19th, 2022, suggesting both anemometers are recording fairly accurate measurements (Figure 2.5). Again, the White Island measurement is typically greater than the Radar Tower measurement. The Radar Tower anemometer is reported to have 1 m/s or 5% error, whichever is larger (Vantage Vue).

Comparison to the National Renewable Energy Laboratory wind resource graph reveals a similar average wind speed as suggested for the region (Figure 2.6).

2.3.2 Measured Power Comparison to Bergey EXCEL 10 Summary Report

Bergey publishes a summary report that shows the results of the turbine power output testing, including a table of hub height wind speed versus expected power output, with combined standard uncertainty. Because measurements of wind speed by both the Radar Tower and White Island anemometers are discretized, plotting individual data points results in unhelpful lines showing what wind speeds are measured by each anemometer. White Island reports wind speed every 10 minutes and the Radar Tower reports wind speed every minute. Thus, 10 minute, 1 hour, and 24 hour averages were considered. A scatterplot comparing the different averagings to the summary report results is shown below (Figure 2.7).

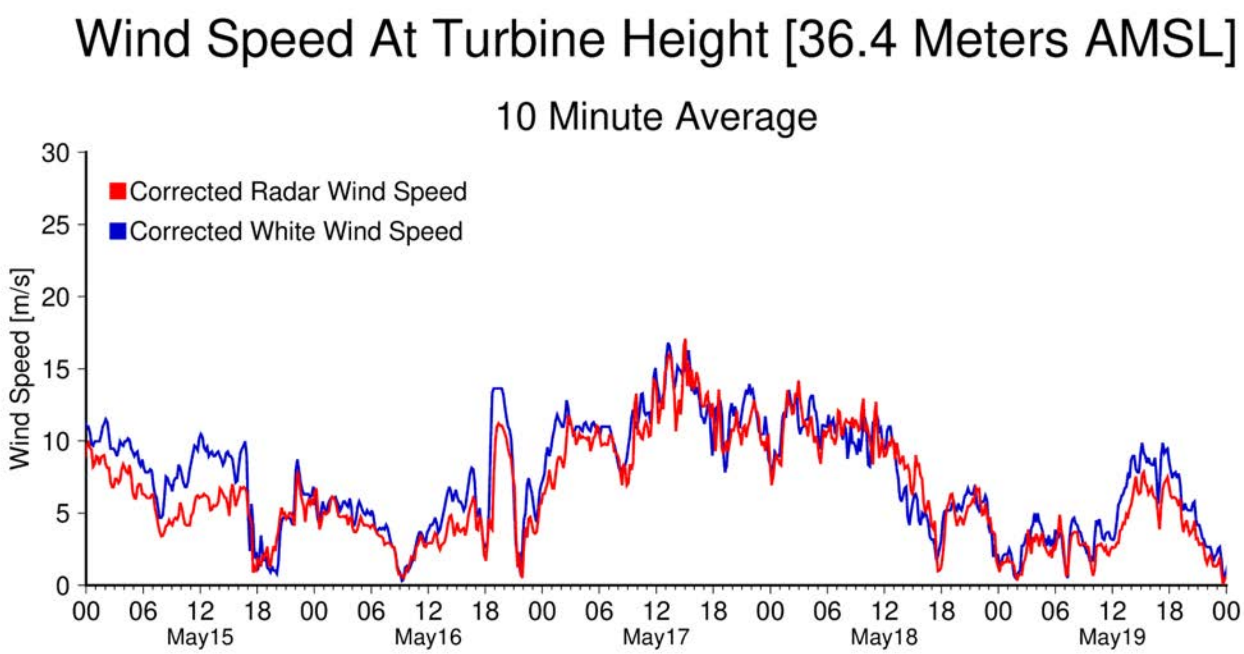

Figure 2.5: Five-day example time series of 10 minute averages of the White Island and Radar Tower wind speeds corrected to turbine height during a range of wind conditions. The White Island wind speed is typically higher, but the two readings closely follow each other.

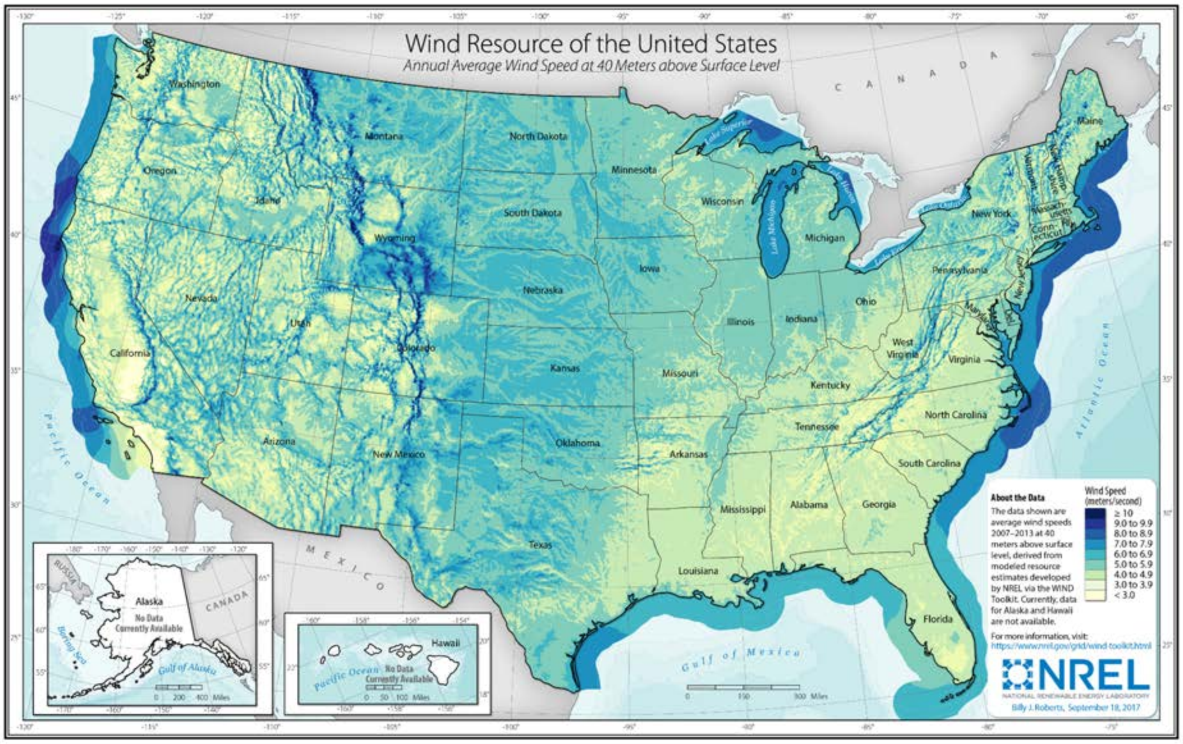

Figure 2.6: National Renewable Energy Laboratory map showing the average wind speed at 40 meters above surface level for the United States. In the Gulf of Maine, off the coast of New Hampshire where the wind turbine is located, NREL reports an average wind speed of 7-7.9 m/s. This is slightly faster than the 6.25 m/s (Radar Tower) and 6.55 m/s (White Island) values calculated, possibly due to the turbine height being 36.4 meters, slightly lower than the 40 meters used in the graph.

2.3.3 Power Sensor Discrepancy

Data for the Bergey VSCII is stored on an SD card within the device. With the help of Tyler Garzo, the interns gained access to the data stored on the SD card on June 22nd, 2022. However, because the VSCII has no internal clock, it stores data in terms of seconds from SD card insertion. Because the time of original SD card insertion was unknown and data only set to record every 10 minutes, the data stored on the SD card from installation until June 22nd, 2022 is not useful. The SD card was set to record every minute and reinserted into the VSCII at 13:49:41 ET on June 22nd, 2022 and taken out at about 08:25 ET on July 1st, 2022 allowing for one week of useful data to compare the VSCII and AcuDC data.

A comparison of the power recorded by the AcuDC and the VSCII, with a linear regression, reveals that the outputs closely follow each other (Figure 2.8). A slope of 0.879 shows that the power readings are correlated, but values of power for the AcuDC tend to be higher than the VSCII.

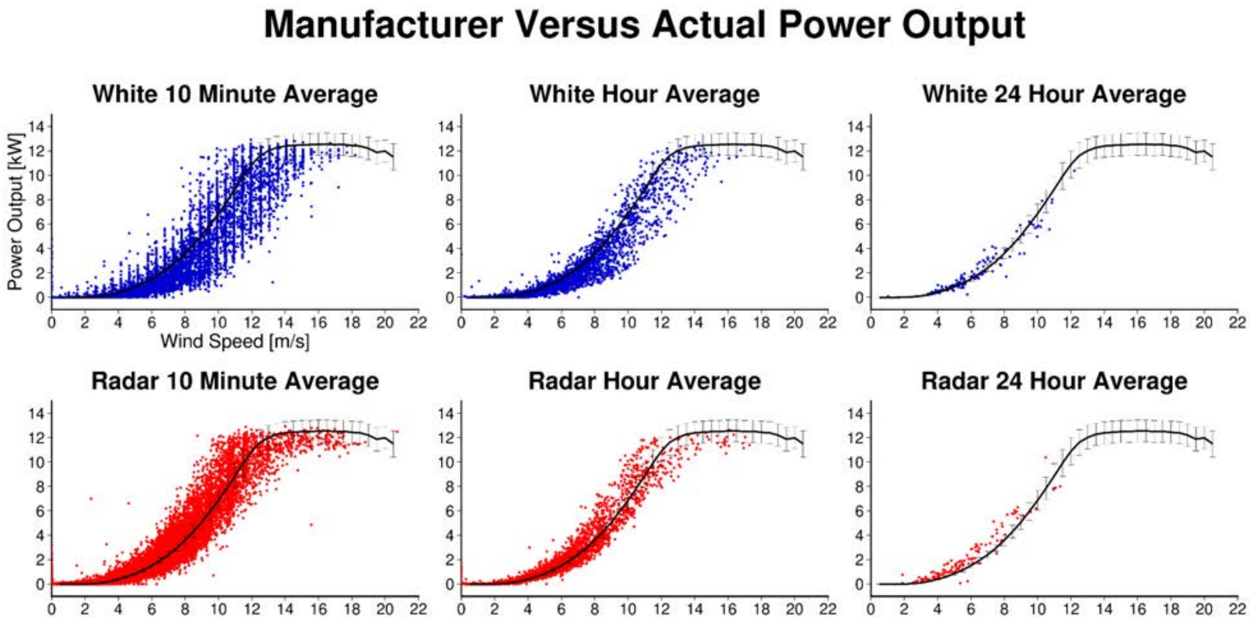

Figure 2.7: Power output versus wind speed. Bergey summary report findings from a 9-month field test are shown as black line with combined error bars. Each sactterpoint represents a 10 minute, 1 hour, or 24 hour averaging of wind speed and output power. The White Island 10 minute plot still has remnants of discretized wind speed readings. As averaging time increases, the data more closely matches what is expected from the summary report. An abundance of nonzero power output points at zero wind speed for the Radar Tower are due to lack of wind speed data at the Radar Tower for that time period. The White Island data falls on and slightly below the summary report curve, while the Radar Tower data falls on and slightly above the summary report curve, as expected for faster wind speeds recorded at White Island. Based on the averaging, the turbine is performing as expected. Lack of extended high speed events make analysis of the upper portion of the curve difficult, but it qualitatively looks to be at or slightly below as expected by the summary report.

To see if there is a qualitative correlation between the power offset and wind speed, both these values were plotted over time. Power offset was calculated by subtracting the VSCII average powers from the AcuDC reading. Of note, the AcuDC data is an instantaneous reading requested every minute on the minute. While it is unclear exactly what the VSCII is reading, it appears to be taking an integral of power over the entire minute to get energy generated over that period. This is especially evident at high wind speeds, where quick fluctuations can make an instantaneous reading very different from a minute average. Because the VSCII only logs energy, it is impossible to get an instantaneous power reading except by looking at the live LCD display on the power controller. Averaging over a shorter time, for example 5 seconds, and taking every twelfth reading may help reduce discrepancies. It appears as those the peaks in wind speed correspond to peaks in power offset (Figure 2.9).

Figure 2.10 shows the difference in readings of the AcuDC and VSCII versus wind speed. This plot has equal amounts of negative and positive offset, likely due to the averaging of the VSCII data. Based on instantaneous readings of both displays, the interns expected the AcuDC reading

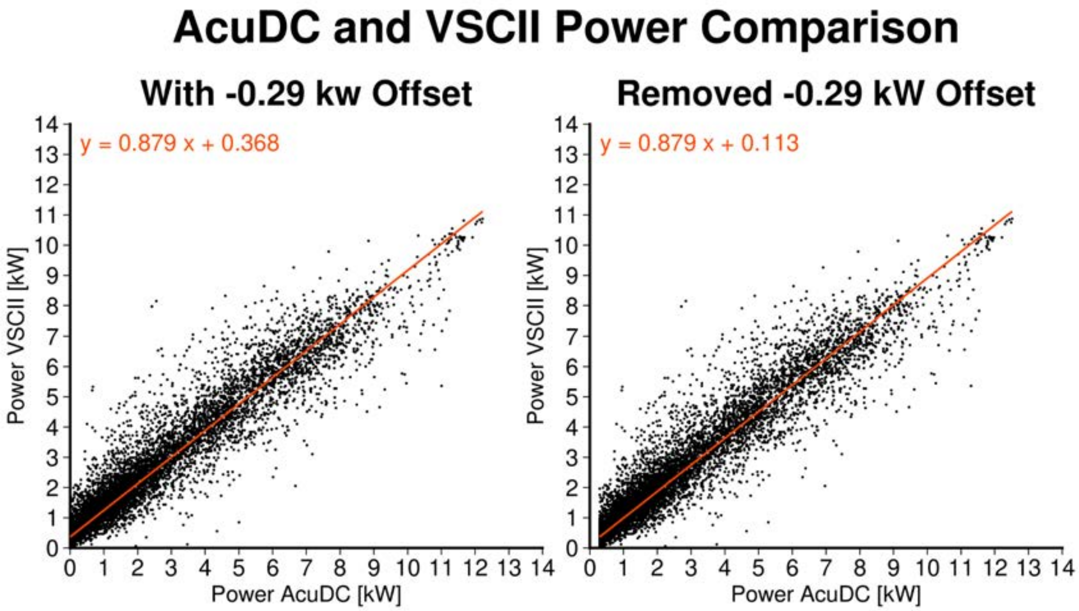

Figure 2.8: VSCII power output versus AcuDC power. Linear regression shows fairly strong correlation between the two ($R^2 = 0.9237$ in both plots). Slope less than one signifies that AcuDC is slightly greater on average.

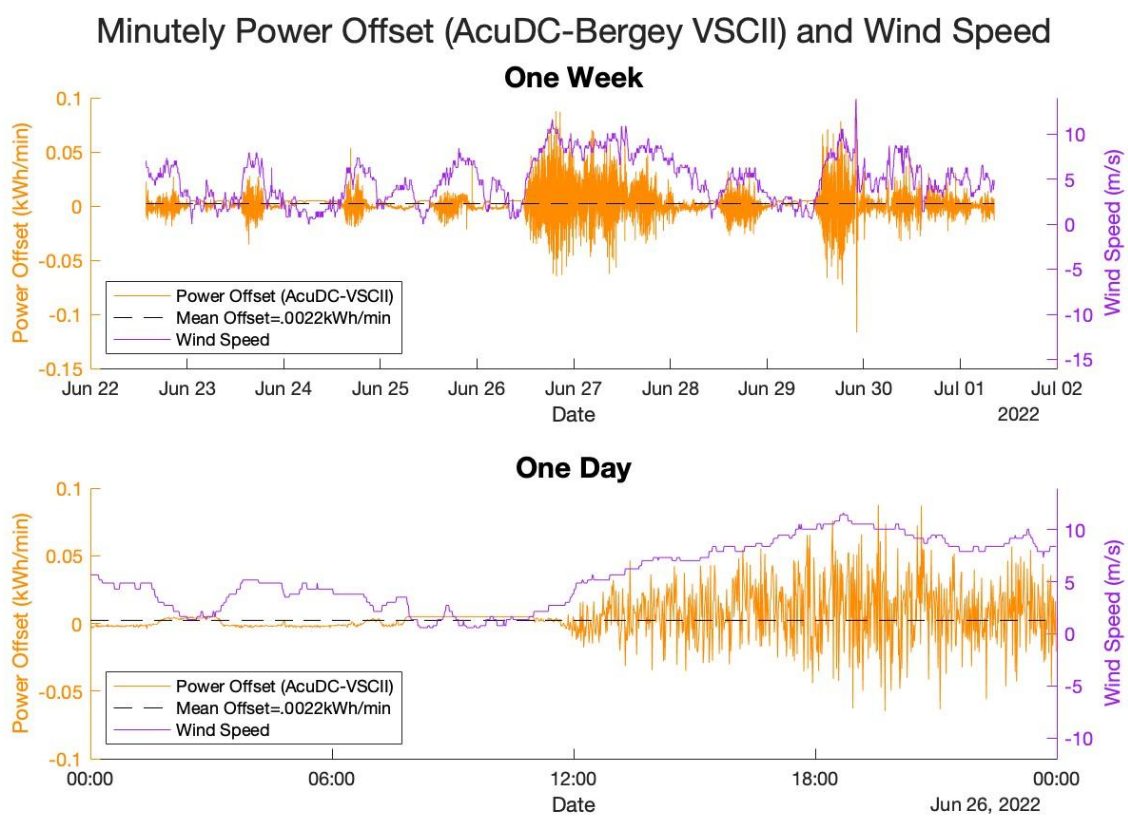

Figure 2.9: Power offset and wind speed over time. Data is plotted every minute. The top graph is over the course of a week. The bottom graph is over one day. Peaks of offset seem to occur when there's peaks in wind speed. The mean power offset is .002 kWh/min, meaning AcuDC is slightly greater than VCSII readings on average.

to always be higher, but due to the averaging this is not the case. Additionally, at high wind speeds, there are sometimes higher levels of offset, but this is not necessarily the case. At high wind speeds there are also instances of no difference at all between the two meters.

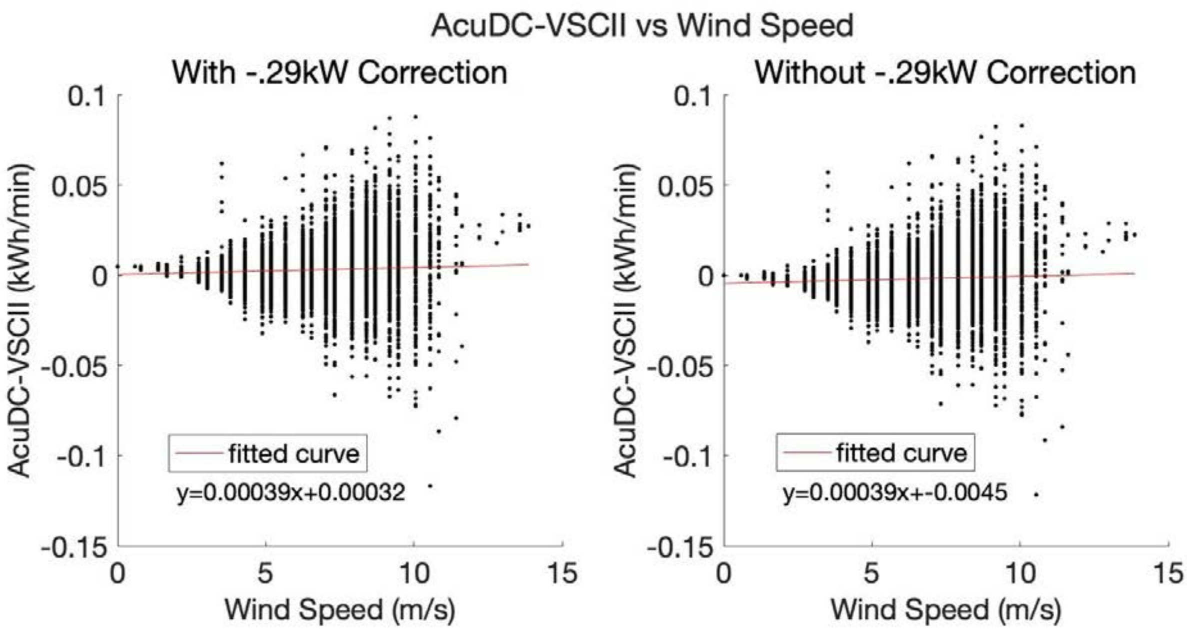

Figure 2.10: Power offset versus wind speed. Positive slope shows that at higher wind speeds offset is slightly higher. Range of offset values increases with wind speed, but there can still be no offset at high wind speeds.

Figure 2.11 shows the cumulative recorded energy generation from the VSCII and the AcuDC, with and without the -.29kW offset. As stated previously, there are about equal amounts of negative and positive offsets, but on average, the AcuDC shows .0022 kW more than the VSCII every minute. While this difference may seem insignificant, over the course of the week, the AcuDC measured a total energy generation of about 28 kWh more than the VSCII did. By dividing this difference by the total number of hours this data was collected over, one can see that the AcuDC overestimates power by an average of .13 kW. Conversely, the current correction of -.29 kW underestimates by about this same amount. Figure 2.12 shows the cumulative energy generation over the week from the VSCII and the AcuDC, this time with an applied offset of -.13kW. Using this offset would result in an equal amount of energy generated at the end of the timeframe we collected data.

2.4 Analysis

Using the discrepancy between White Island and Radar Tower corrected wind speed as a guide, the interns believe a power law wind speed relationship with $\alpha = 0.1$ provides a reasonable measurement of the wind speed at hub height using either data set. There is no reasonable value of α that produces no discrepancy due to the lower elevation anemometer having a faster typical wind speed, suggesting that other factors not accounted for by a simple power law are present.

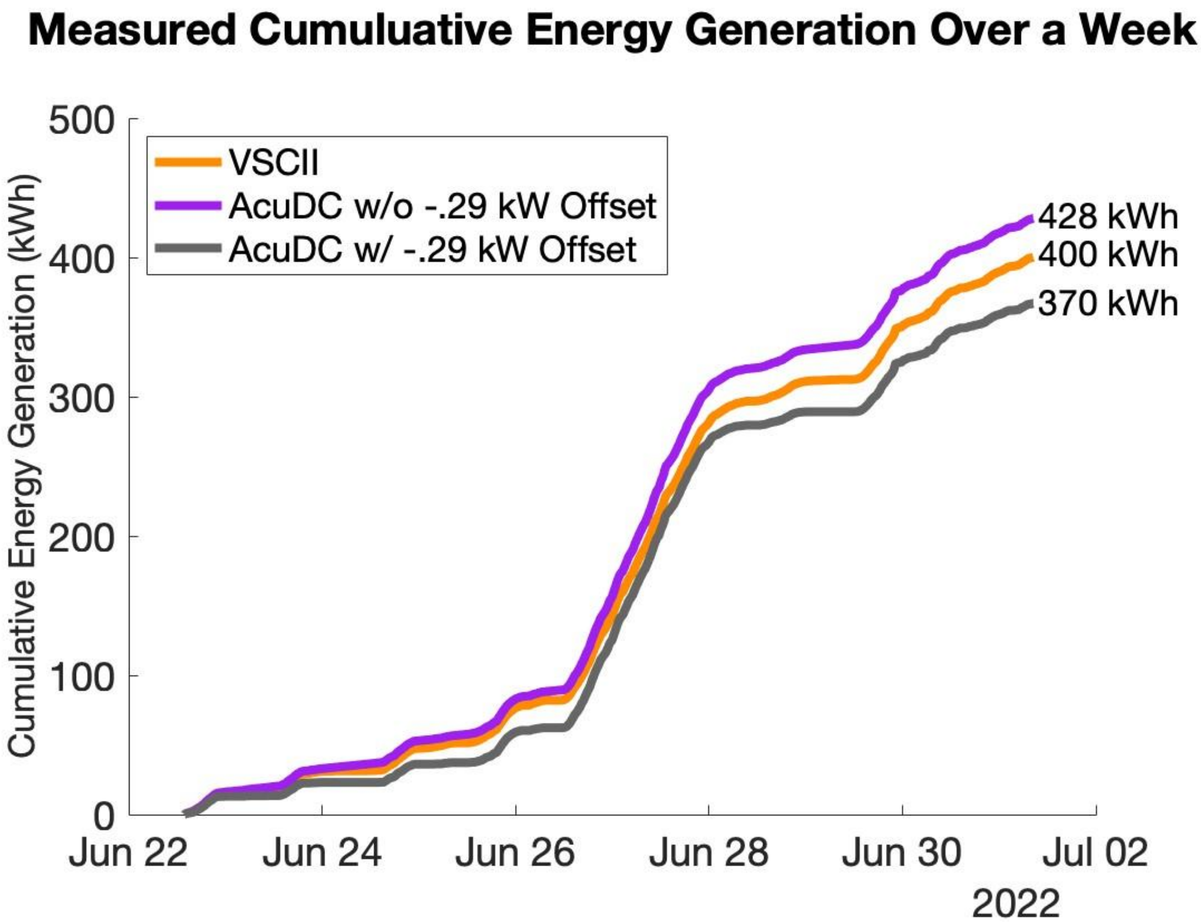

Figure 2.11: Cumulative energy generation over the course of a week of VSCII and AcuDC, with and without the -.29 kW correction. AcuDC raw data overestimates energy generated, while the Dashboard underestimates how much energy generated..

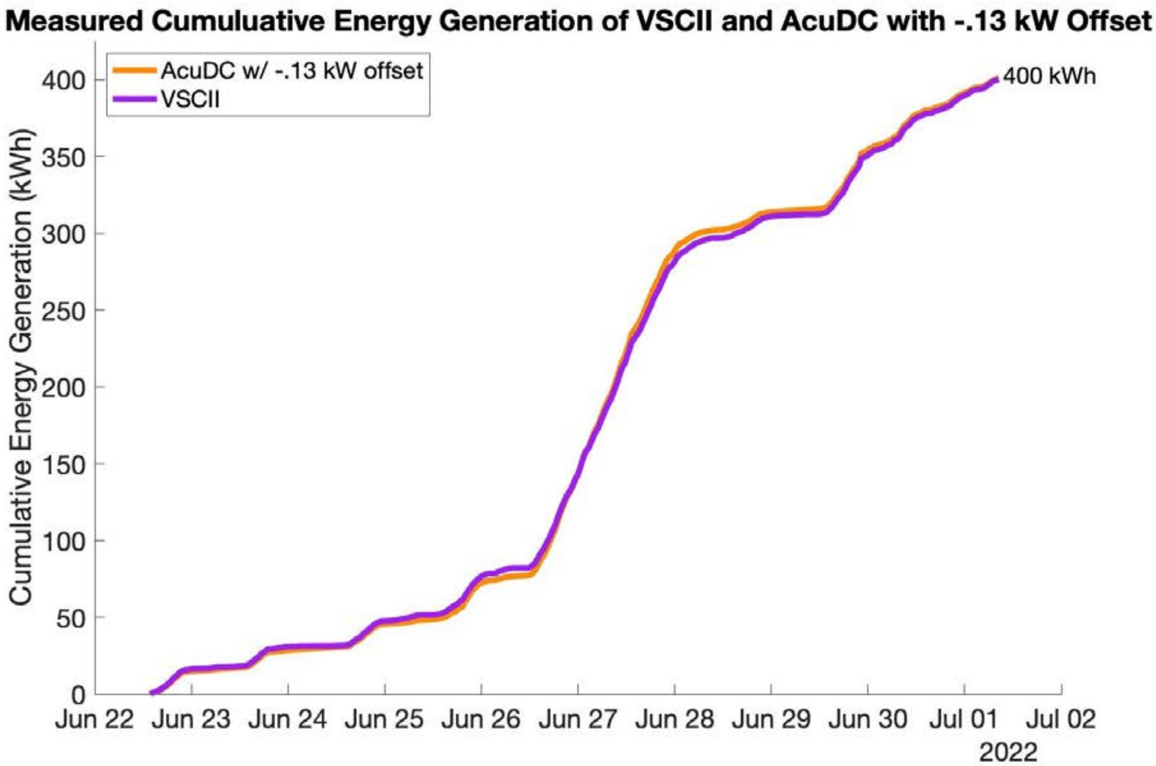

Figure 2.12: Actual energy generated over the week from VSCII and the AcuDC energy generated with recommended -.13 kW correction. At the end of the week, both sets of data total the same amount of energy generated

Because power scales with the cube of the wind speed, having an accurate wind speed at hub height is extremely important for obtaining accurate power estimates.

The measured power comparison to Bergey EXCEL 10 Summary Report shows that the turbine is generally performing as expected. Although an average of 10 minutes produces very scattered data, longer averaging times produce a plot that closely follows the curve given in the Summary Report. Many data points fall outside the given standard error by the Summary Report, but this is expected due to the error accumulated in estimating the wind speed at hub height.

The power sensor discrepancy analysis shows that better data needs to be collected to make an informative conclusion about the relationship between the two sensor readings. Because the two sensors are directly connected to each other, a reasonable explanation for the discrepancy is sensor calibration. The interns ran brief experiments to see what could be affecting the AcuDC meter. When the VSCII charge controller was turned off, which halts wind power from coming into the grid, the AcuDC still displayed a baseline power production. This number hovered around 1.25 kW. To see if solar production had an effect on the readings, the interns had Ross open the solar circuits so that they were no longer connected to the AcuDC. With the VSCII turned off, this resulted in a negligible change in AcuDC meter. This suggests that solar production does not have an effect on the meter offset. Based on results from the 2021 SEI, the idea of finding a relationship between wind speed and offset was investigated. Plotting both power offset and wind speed on the same graph over time suggested there might be a direct relationship that could be found. Plotting the power offset at each wind speed showed a clear relationship might not be possible to formulate. There were many instances where higher wind speeds induced higher power offsets, but this was not necessarily the case for all meter differences at high wind speeds. There were also many instances where there was no difference at a high wind speed. So while the range of possible offset values increases with wind speed, there is no way to formulate an equation that suggests a proper offset at specific wind speeds as suggested by the 2021 SEI group.

2.5 Conclusions and Recommendations

The adjusted value of 43 m for the Radar Tower seems significantly more accurate compared to the 54 m value previously used. However, when adjusted to hub height there was still a difference between wind speed data from the Radar Tower and White Island. The interns recommend further study of the discrepancy in wind speeds between the White Island and Radar Tower anemometers. Possible causes of discrepancy may include complex interactions with Appledore Island topography, eddies from the camera mount on top of the radar tower, and prevailing wind direction in comparison to the Isle of Shoals archipelago layout.

While the interns were able to collect more data points than previous interns by getting access to the SD card in the VSCII, still no definitive conclusions could be drawn. If future interns should continue to study the discrepancy between the AcuDC and VSCII readings, then the interns recommend that the current offset of -.29 kW continue to be used on the dashboard. The data collection did show that this -.29 kW offset did not settle the discrepancy, and in this case even made it worse. Despite this, interns still recommend keeping it so that all past and future data has the same offset. Hopefully this continuity in data will make future data analysis more straightword. Interns believe the discrepancy may be due to how the meters display average power readings vs. instantaneous power readings. Depending on whether the wind speed is increasing or decreasing over the minute, the offset may be positive or negative. Further studies should attempt to use a shorter interval time with the VSCII. This way, a shorter and more accurate average power can be used to compare to the AcuDC instantaneous power readings. For example, one could calculate the average power based on energy generated a few seconds before and after each minute the AcuDC displays instantaneous power. Interns could also try to use OCR technology, with the help of Tyler and his cameras, to read the instantaneous power from the LCD display of the VSCII. This way, a useful trendline similar to Figure 2.8 can easily determine the best way to correct the data so the dashboard displays the most accurate data. The SD card was replaced into the VSCII at 08:30:03 ET on July 1st, 2022, and set to output the power at 60 second intervals, in sync with the readings of power from the AcuDC on the dashboard. Overall, having more data will help better constrain the relationship between the two readings.

If, however, future research is determined not to be worth pursuing, then the interns recommend an offset of -.13kW be applied to AcuDC data to be displayed on the dashboard. While this offset might not display the exact instantaneous power output of the turbine accurately at any given moment, the goal would be to have an accurate measurement of total energy generated over a period of time. With this offset, the total energy generated over the week we measured came out to the same value. Hopefully, this offset would make values of energy generation over a month or a year match up as well. This offset also coincides with the .125kW value the interns observed displayed on the AcuDC when the VSCII was turned off. This offset should provide more accurate data that is indicative of how the island is performing in terms of sustainability, i.e. how much green energy is generated over the course of a season.

2.6 References

Bergey Windpower Company Excel 10 Wind Turbine and Powersync II Grid-Intertie Inverter, Revision 2.1, August 2020

Bergey Windpower Company Excel 10 SWCC Summary Report, Solar Rating and Certification Corp, 2017

Elzweig, Brooke Lynn, Robarts, Zachary, *Sustainable Engineering Internship 2021 Final Report*, 30 August 2021.

Kim, Yong-Hwan, Lim, Hee-Change, *Effect of island topography and surface roughness on the estimation of annual energy production of offshore wind farms*, Renewable Energy, 12 November 2016.

National Data Buoy Center, *Station IOSN3 - Isle of Shoals, NH*, NOAA

Wosnik, Martin, Wind Energy, *Wind Energy Resource*, Wind Energy Lectures Part 3, 11 September 2019.

Vantage Vue Weather Station, *Specifications Sheet*, Sensor Suite Model 6537

VCSII – Battery Charger Bergey WindPower Co. Owner’s Manual, 17 June 201

3 Drinking Water Life Cycle Analysis

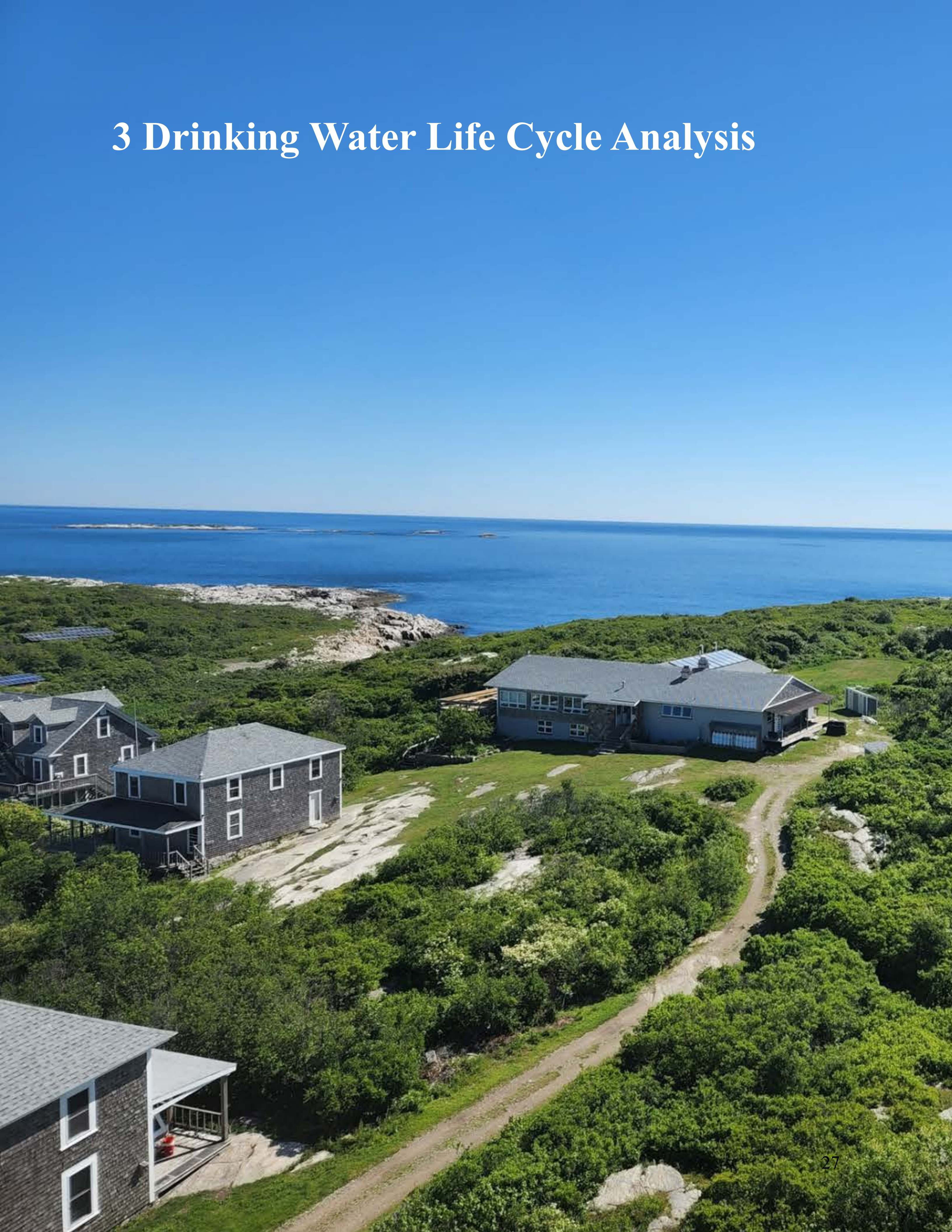

Lead Interns: Tess Hays, Zachary Katz, Izzy Medeiros, Jason Shao

3.1 Background

Appledore Island has a drinking water system that is dependent on both a freshwater well and a reverse osmosis (RO) system that desalinates incoming seawater. The system consists of a 20 feet deep fresh water well, a reverse osmosis machine, a chlorine disinfection system, a cistern that stores the clean water, and a pressure tank for distribution. The reverse osmosis system runs using solar energy once the grid batteries are fully charged, allowing it to take advantage of available renewable energy instead of fossil fuels. A significant amount of energy is consumed by pumps: seawater is pumped to the reverse osmosis system, chlorine is pumped into the cistern to disinfect water from both the well and the reverse osmosis system, and the stored water is pumped from the cistern to the pressure tank. The Shoals Marine Laboratory would like to assess how sustainable the drinking water system actually is, so a life cycle analysis was conducted to determine the equivalent carbon emissions from the entire system.

3.2 Purpose

In order to evaluate how sustainable the drinking water system actually is, a life cycle analysis was conducted. A life cycle analysis is a study of the assembly, transportation, use, maintenance, and disposal phases of the components in the system to assess the environmental impact of the system holistically (Figure 3.1). In this analysis, SimaPro was used to input the materials and energy used throughout the lifecycle of both the reverse osmosis and well drinking water systems. By using SimaPro, the equivalent carbon emissions of all life cycle stages for each component of the drinking water system was calculated and analyzed.

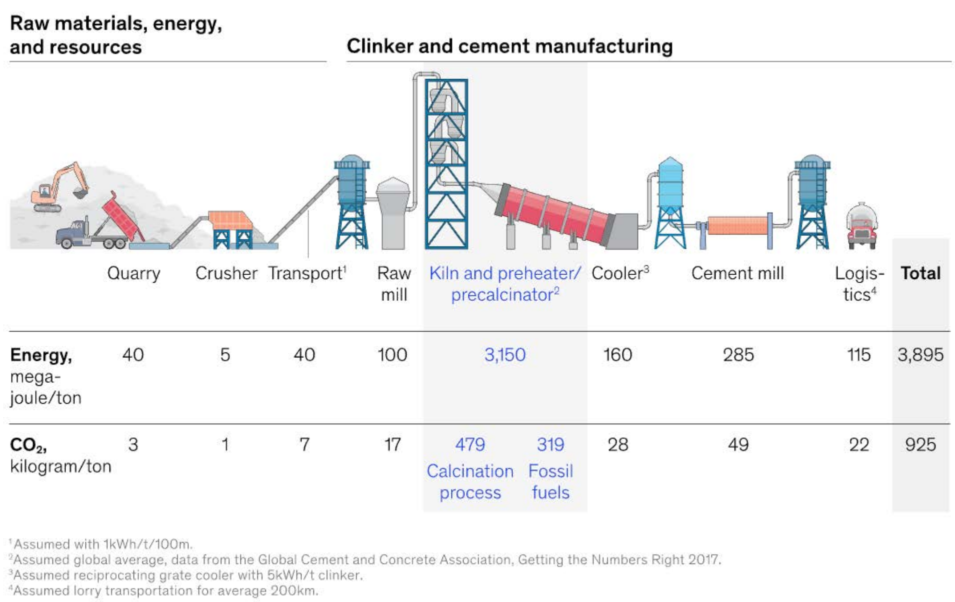

Figure 3.1: Example processes and assumptions considered when thinking about the assembly and transportation phase of cement. A life cycle analysis also looks at the use, maintenance, and disposal phases of the product.

3.3 Scope

Each aspect of the life cycle for every material must be considered for an accurate assessment of the entire system. In the first stage, manufacturing and assembly, the interns observed and researched the various materials that comprise the reverse osmosis machine, well, cistern, pressure tank, piping, and pump systems. In addition, the transportation of these materials to be assembled as well as the transportation of the materials to the island were considered. In the next phase, the use phase, the energy intake of each system component was calculated and considered, as well as how long each part lasts until replacement. During the maintenance phase, the materials and energy needed to maintain the systems was determined. Lastly, the disposal phase accounted for what will happen to each material once they exceed their lifetime.

3.4 Methods

3.4.1 Data Acquisition

In order to determine the total equivalent carbon emissions that manufacturing contributed, all the materials that comprise the system had to be taken into account. Components of the drinking water system that could be accessed were measured directly, while the lengths of underground piping were estimated using Google Maps. Knowing the manufacturer and model number of the RO, information on the materials could be found online. A flowchart of SML's freshwater system is shown in Figure 3.2.

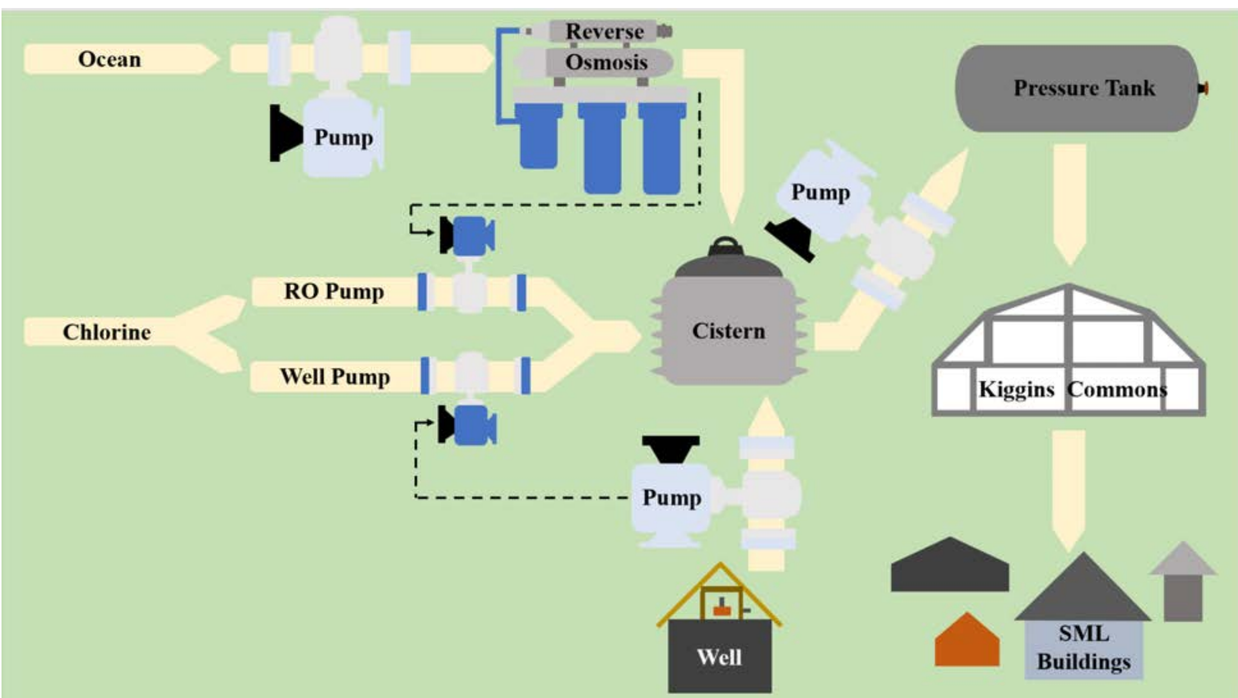

Figure 3.2: Flowchart of SML's freshwater system. Saltwater is pumped from the ocean and processed in the reverse osmosis machine before entering the cistern as freshwater. Freshwater from a 20 foot dug well is also pumped to the cistern. Two chlorine pumps, controlled by the amount of water being pumped from the reverse osmosis machine and well, treat the water. The cistern water is pumped to a pressure tank and the pressurized water flows uphill to Kiggins Commons and the other SML buildings requiring freshwater.

The power demand of the several pumps and motors in the system was determined by using a meter to measure the average instantaneous power demand of the pumps. Knowing the average time the pumps were active during the day, the interns calculated the total amount of energy expended during the use phase of the system. Since about 20 percent of the island's energy is produced by combusting diesel, the energy used by the pumps was able to be converted into diesel use. The RO is manually turned on when the forecast shows plenty of sun for solar power generation. Thus, The RO is essentially run entirely on the green grid, and the carbon emissions from operation were not considered.

To figure out the extent of maintenance required, the interns questioned the engineers on the island who manage the system day to day. Infrastructure that was on the island before the establishment of SML, such as the well, has no major maintenance needs. Pumps were assumed to have a lifetime of about 10 years. Pumps used on the island have been operational for over 25 years, so this estimate is conservative. The polyethylene pipes which transport the water throughout the island have an average lifetime of about 45 years. A significant amount of maintenance is required for the RO. Membranes in the machine must be replaced on a yearly basis. Additionally, the RO must undergo a yearly oil change. After a component has reached the end of its usable lifetime, all parts that cannot be sold to a scrap yard will be disposed of in a landfill.

To compare the current drinking water system to an alternative, the interns also measured the equivalent carbon emissions of producing water containers and transporting them to the island in order to meet the fresh water needs of the island. Because SML uses an average of 1000 gallons of water per day, seasonally dependent on island population, the analysis assumed bringing 1000 gallons of municipal water to SML in 250 gallon plastic jugs daily.

3.4.2 SimaPro

Once all the data was collected and compiled, SimaPro was used to calculate the equivalent carbon emissions associated with the life cycle of the entire drinking water system. SimaPro takes into account raw material extraction, manufacturing, energy used by the components of the system, how long they last, and how they will be disposed of. SimaPro then looks at all associated emissions and converts it into a single value of kg CO_2-eq. This is calculated based on the 2021 IPCC Global Warming Potentials, which measure how much energy 1 ton of different gasses absorb compared to an equivalent amount of CO_2, in this case on a 100 year timescale. SimaPro splits this value into fossil fuel, biogenic, and land transformation emissions. Because of SML's unique island environment, the interns had to separately calculate the carbon emissions associated with transporting materials to and from the island using the Kingsbury or Heiser, assuming an average of 20 gallons of diesel per round trip (Figure 3.3).

Component	Material	Explanation	Value	SimaPro Input
Well	Concrete	Octagon Base of Well	100 ft^3	Concrete, medium strength {RoW}| market for concrete, medium strength | APOS, U
	Tin	Well Sides	4300 kg	Tin {GLO}| market for | APOS, U
	Polypropylene	Well Roof	7.75 kg	Polypropylene, granulate {GLO}| market for | APOS, U

SimaPro Outputs (kg CO2-eq)					
Fossil	Biogenic	Land Transformation	Total	Lifetime (Years)	Assumptions and Comments
983	1.38	0.782	985.16	75	From measurement of well (Octagon minus circle); Assumed medium strength concrete
43100	72.8	69.6	43200	60	From measurement of well, pi * (39/12)' ^2 * 20 ft; Assumed 3/8" thickness and density 7.31 g/cm^3
18.2	0.0243	0.00742	18.232	25	From measurement of well, double layered; 80" * 51" * 2 (sides) * 2 (sheets per side) *.032in thickness. Assumed corrugated plastic made of polypropylene

Figure 3.3: Example inputs to and outputs from SimaPro extracted from the full life cycle analysis spreadsheet (See supplementary material). For each input, the amount inputted into SimaPro was calculated, lifetime estimated, and assumptions listed. The given input was used in SimaPro to produce the carbon dioxide equivalent outputs. This example is just for a small portion of the manufacturing portion of the well; in the full analysis all components and use phases were considered.

3.5 Results and Analysis

3.5.1 General Findings

It was found that the life cycle of the freshwater system would release the carbon dioxide equivalent of 2935872 kg into the atmosphere. The stainless steel pressure tank resulted in the largest overall carbon dioxide equivalent production due to the emissions from fossil fuels in the manufacturing phase of the life cycle analysis. The tin for the well, another metal component, largely contributed to the equivalent carbon dioxide emissions.

Figure 3.4 shows the total emissions of the drinking water system over a lifetime of 100 years, split by both system component and life cycle stage. Figure 3.5 shows the relative emissions of the drinking water system over the same lifetime of 100 years, split by both system component and life cycle stage.

3.5.2 Comparison

Figure 3.6 shows the total emissions of the current drinking water system compared to the imported water equivalent. This scenario assumed one additional boat trip to the island with four 250 gallon jugs of water, similar to how White Island has dealt with water needs in the past.

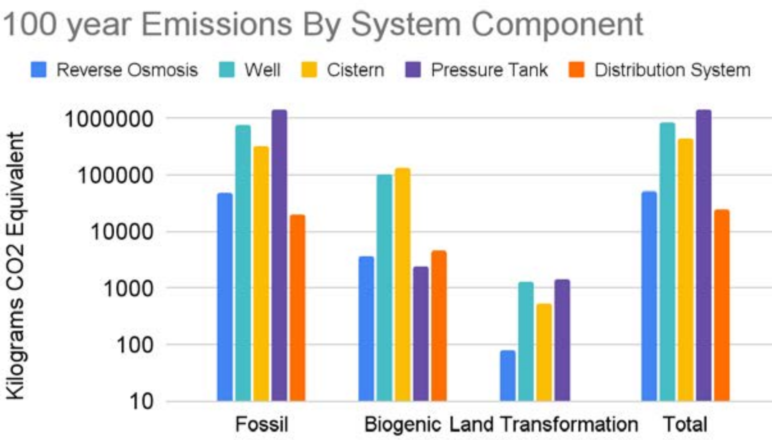

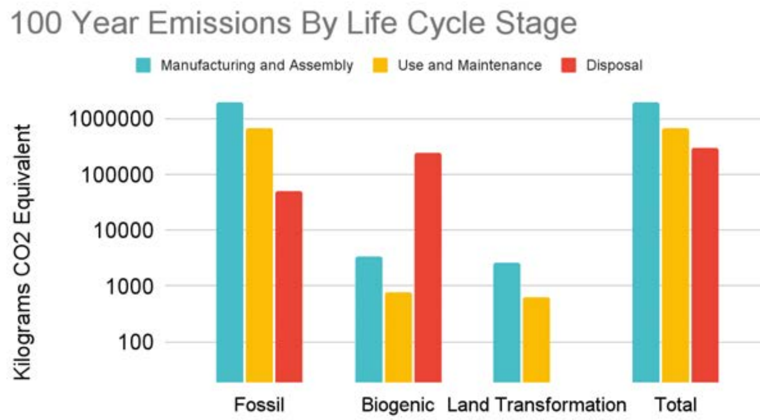

Figure 3.4: Fossil, biogenic, land transformation, and total emissions for a 100 year life cycle analysis of SML's drinking water system, by system component (left) and life cycle stage (right). Fossil emissions are typically the largest component of emissions over any component and life cycle stage. Total emissions from the well and pressure tank are largest, due to the large amount of metal used in their construction; this also inflates the manufacturing and assembly emissions. A small use and maintenance emissions means that as the system continues to operate for longer, it becomes more sustainable

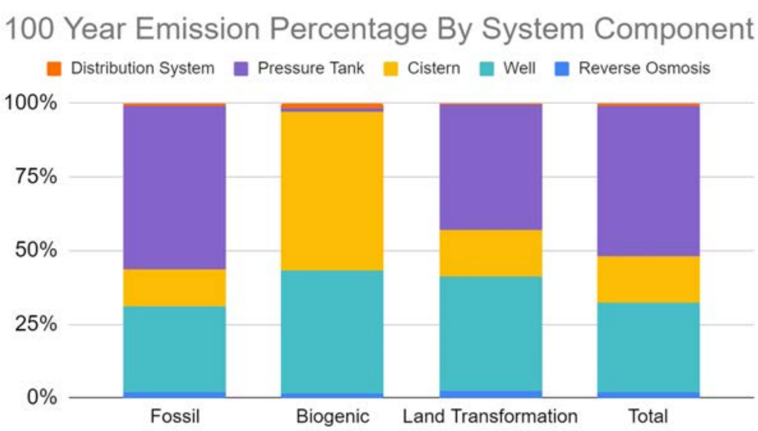

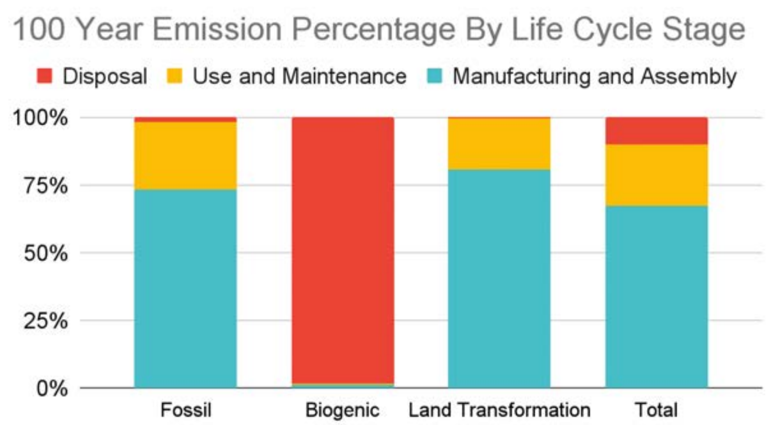

Figure 3.5: Fossil, biogenic, land transformation, and total emissions percentages for a 100 year life cycle analysis of SML's drinking water. Total emission percentages from the well and pressure tank are largest, due to the large amount of metal used in their construction, but the cistern has a large biogenic impact. Disposal produces most of the biogenic emissions, due to organisms in the landfill.

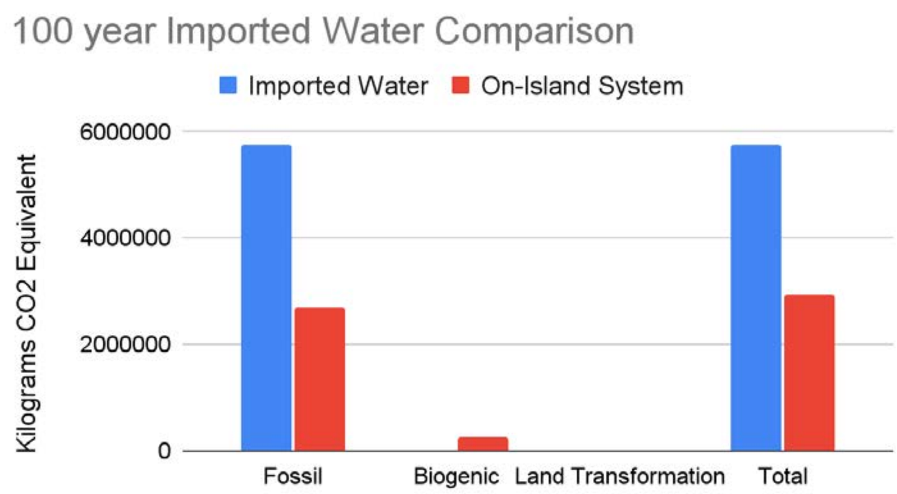

Figure 3.6: A comparison between the current freshwater drinking system and importing water shows importing has almost twice the emissions over a 100 year time span. Because most of the emissions of imported water come from the use phase, boating it over to SML, compared to the manufacturing phase in the current system, the imported water system becomes worse the longer it is used.

3.6 Conclusions and Recommendations

Though the system as analyzed is sustainable, there is some error associated with the analysis that must be noted. To use SimaPro, assumptions must be made about the materials used during the manufacturing phase, as some materials the interns noted were not in the SimaPro database. The inputs for this phase can be found in Appendix C. Small details, such as nuts and bolts used to secure the pumps on their plywood platform in the cistern shed were omitted, as their amounts would be so small that they would not greatly impact the SimaPro output. Lastly, estimations were made to approximate the lengths of piping used throughout the island, as these pipes are underground and it would be unrealistic to dig them up for the purposes of this analysis. A recommendation for maintaining the sustainability of the system is to consider environmental impact when selecting replacement materials. For example, metal components had a much higher carbon footprint than plastic components. Additionally, using existing components is better than producing new ones.

After analyzing the life cycle of the existing drinking water system, it was difficult to determine the sustainability of the system without making the comparison of how the island used to obtain potable water, shown in Figure 3.6. Once this comparison was made, it became evident that the drinking water system here on Appledore is a much more sustainable solution than the alternative. By importing water, the equivalent carbon dioxide equivalent is almost double that of the on-island system. Additionally, the well and cistern were here before the establishment of SML. This made producing new components unecessary. The longer the system lasts, the more sustainable it becomes, as the system continues to benefit the island without constantly needing new materials; they already exist here.

3.7 References

Feng, Danyi, Song, Cuihong, Mo, Weiwei, *Environmental, human health, and economic implications of landfill leachate for per- and polyfluoroalkyl substance removal*, Journal of Environmental Management, 12 April 2021

Guglielmi, G.; Mitchell, B.; Song, C.; Kinsey, B.L.; Mo, W. *Life Cycle Environmental and Economic Comparison of Water Droplet Machining and Traditional Abrasive Waterjet Cutting*. Sustainability 2021, 13, 12275. https://doi.org/10.3390/su132112275

Lifestream Watersystems, https://www.lifestreamwater.com/.

Mo, Weiwei, *Introduction to Life Cycle Assessment*, Lecture, 28 June 2019

Mo, Weiwei, *LCA Example - Concrete vs Clay tiles*, Lecture, 29 June 2019

Mo, Weiwei, *SimaPro introduction*, Lecture, 29 June 2019

4 Engineered Erosion Control

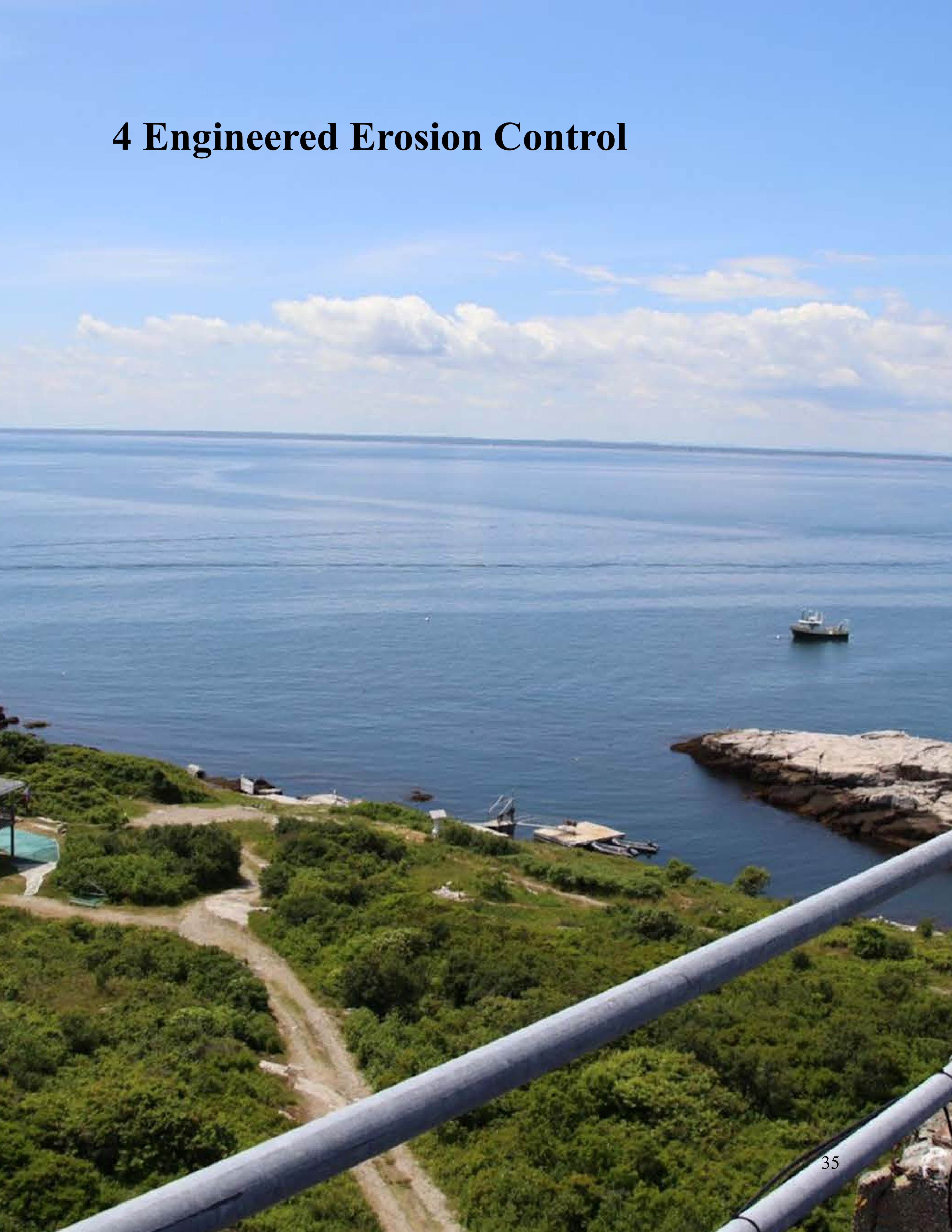

Lead Interns: Tess Hays, Izzy Medeiros

4.1 Background

Stormwater erosion has a large impact on the roads at Appledore. Though there are many walkable paths, it is crucial that Appledore maintains its drivable roads to continue to transport materials and people around the island. Shown in Figure 4.1 below is an example of the damage erosion has caused in an area referred to later in the report as Site 1.

Figure 4.1: Erosion after storm surge

Off-season storm damage on the island is more severe than storm damage that occurs in the summer. Storm surges allow for waves to access higher elevations, causing erosion at higher elevations than that of summer storms. Though hurricanes and tropical storms may not reach the Isles of Shoals directly, waves from these storms can and have caused severe erosion (Birchler, 2014). As global climate change continues to increase the severity of storms, it is critical that there is strong infrastructure in place to protect the roads from damage. Some forms of erosion affecting the roads cannot be fixed with additional fill. In one area of study, a winter storm carved out part of the edge of the roadway along the western coast shown in Figure 4.2, where any more erosion would prohibit vehicles from driving on this roadway.

Figure 4.2: Erosion caused by winter storm damage

The roads are filled with finer gravel material that becomes washed out with water flow during a storm. When walking along the roads, evidence of erosion is present where there is larger aggregate, as the finer material has been removed by water flow, shown below in Figure 4.3.

Figure 4.3: An eroded area of road

4.2 Purpose

For a remote island location, it is expensive and inefficient to replace fill that washes away. Controlling this erosion can protect the roads of Appledore and save the island material and labor costs. In low water flow (observed 6/17/22) water collects in lower areas of the road, and follows the natural contour of the roadways. The interns were tasked with preventing wear on the roads caused by erosion by thinking of ways to divert or control flow.

4.3 Scope

Since water flows from high to low elevations, an elevation survey of the roads on higher elevations was conducted. By protecting higher elevations, water flow can be prevented from flowing down to lower elevations, which could save the amount of fill that would otherwise get washed away. The purpose of these elevation surveys was to create a profile of each slope, which would then allow the interns or island staff to determine the areas of highest concern. In addition, a horizontal profile of each site was conducted to observe the rutting that occurs in these roads. The interns chose an area that was representative of the conditions of the slope, and then conducted another elevation survey for all five sites.

The loop shown in Figure 4.4 was studied in five different sites of the steepest slopes of the island roads. Site 2B is on the same slope of Site 2, but due to the turn in between sites, it was split into two sections.

Figure 4.4: Erosion sites, Appledore Island 2022

4.4 Methods

4.4.1 Individual Site Surveying

Interns took to the field to manually survey the elevation of the erosion sites. For these elevation surveys, both a transit and measuring rod system were used, starting with the lower points of elevation. The transit was situated at a station point and from this station, elevation measurements read off the rod through the transit were recorded at horizontal intervals. From this data, both the horizontal run and vertical rise were obtained to calculate the slope of each site. This information allowed for a comprehensive evaluation of each erosion site, and contributed to more in depth suggestions for erosion combative techniques.

4.4.2 Calculating the Amount of Fill Needed

To calculate how much fill will be needed at maximum, the interns first considered the horizontal profile of each site. A foot of each end of the profile was not included in the fill calculations, as these individual foot measurements were a measurement of the grass on either side of the road. After speaking with Jacob Shactman, a civil engineer at Wright-Pierce, the interns created a "crown" profile, an example shown in Figure 4.5, with half an inch slope and existing grade tied in on either side. The "crown" shape would ensure that rainwater immediately flows off the road. The area between the "crown" and the existing road grade was then estimated by using triangular and rectangular shapes. Once this area was obtained for each site, it was then multiplied by the length of the slope to calculate an approximate amount of how much fill would be needed throughout the slope. This option is available should island staff choose to fill in all of the roads.

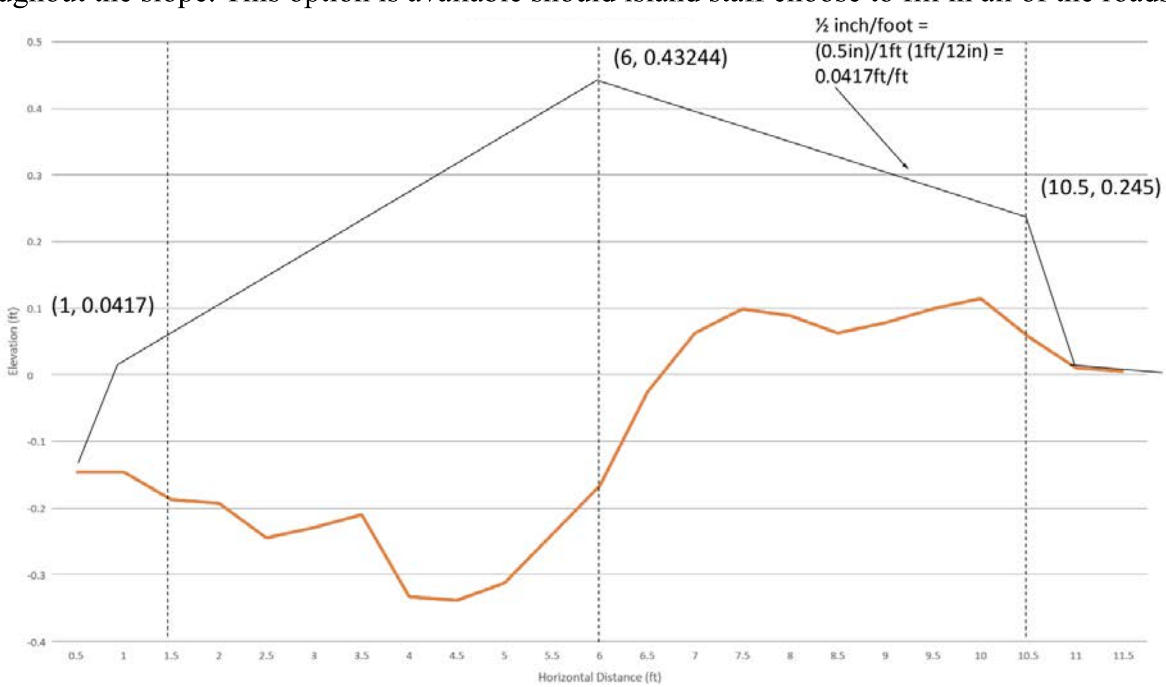

Figure 4.5: Site 1 Horizontal Profile

To calculate the minimum amount of fill needed to return the roads to a good condition, a line from the highest elevation of the horizontal profile (excluding the edges of the road) was drawn across the profile for each site. Figure 4.6 shows that the profile was then divided into sections of similar shapes in order to approximate the area between the existing elevations and the horizontal line drawn across. The areas of these sections (Table 4.1) were then added together and multiplied by the minimum distance that should be filled. The minimum distance was determined by the interns in the field, measuring the lengths of the areas with the worst conditions. This would allow the interns to analyze how much fill would be needed if the island staff wish to fill in the more dire areas, as opposed to creating a crown along the whole slope.

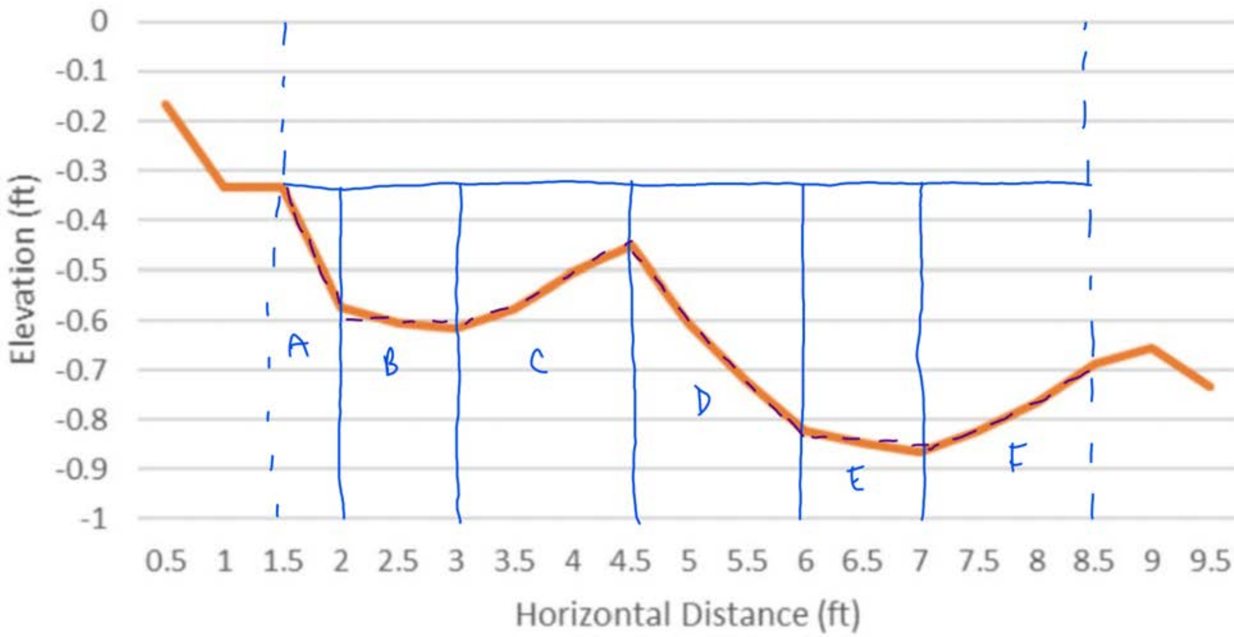

Figure 4.6: Flat Fill Site 2B

Table 4.1: Area Breakdown for Fill, Site 2B

Section of Profile	Area (ft^2)
A	0.05
B	0.25
C	0.26
D	0.41
E	0.5
F	0.8
SUM (ft^2)	2.27

4.5 Results and Analysis

4.5.1 Soil Survey Results

A soil survey was conducted through the USDA and NRCS website, the results of which were used to determine soil classifications and thus more effective erosion treatments.

Map Unit Legend

Map Unit Symbol	Map Unit Name	Acres in AOI	Percent of AOI
Ch	Chocorua peat	1.5	0.8%
LyB	Lyman-Rock outcrop complex, 3 to 8 percent slopes	18.3	9.4%
LyC	Lyman-Rock outcrop complex, 8 to 15 percent slopes	20.1	10.3%
LyE	Lyman-Rock outcrop complex, 15 to 80 percent slopes	5.2	2.7%
RoC	Rock outcrop-Lyman complex, 3 to 15 percent slopes	24.1	12.4%
RoE	Rock outcrop-Lyman complex, 15 to 80 percent slopes	27.8	14.2%
W	Water bodies	98.1	50.3%
Totals for Area of Interest		**195.2**	**100.0%**

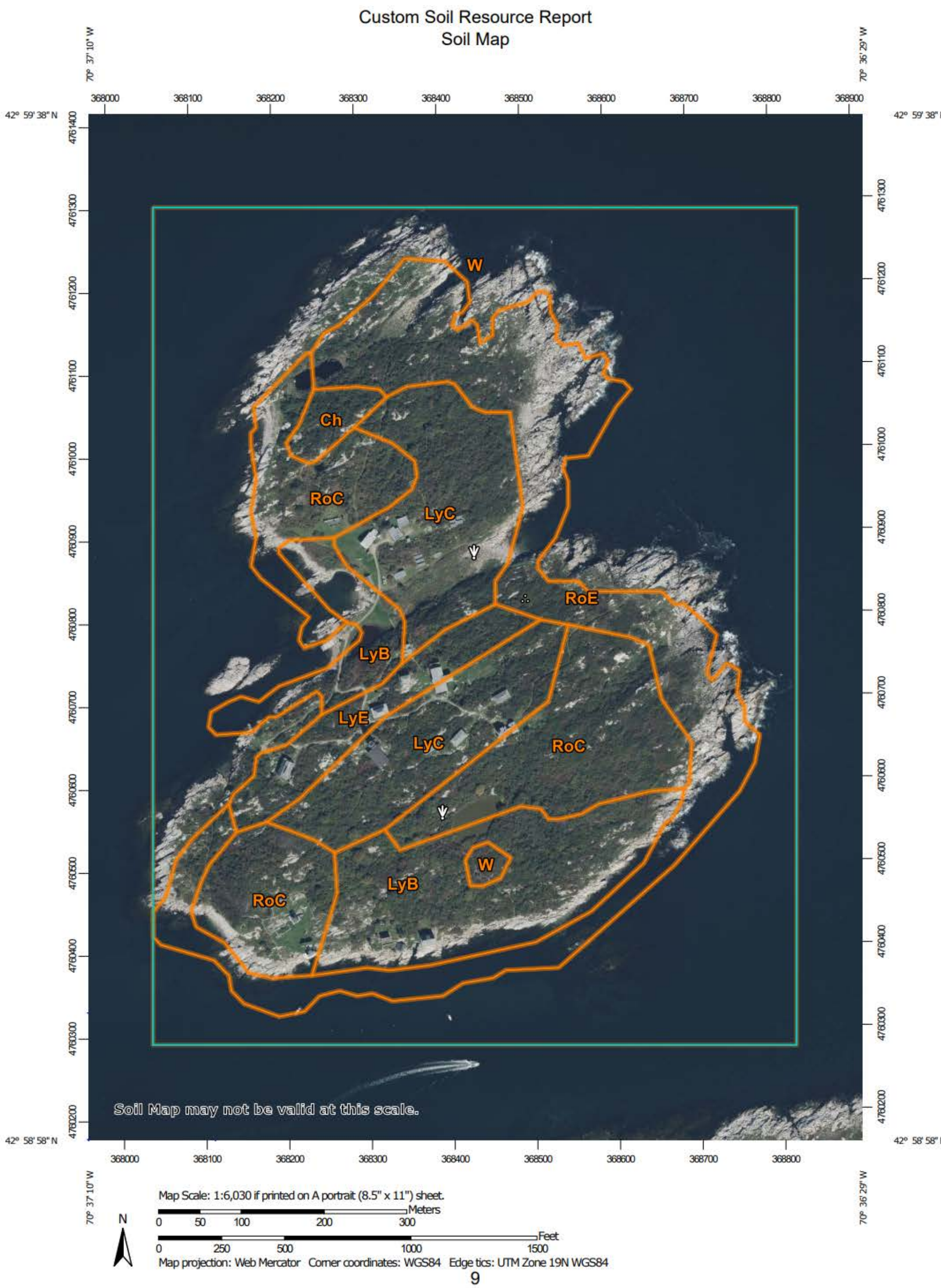

Figure 4.7: Soil classifications for Appledore Island.

4.5.2 Site Information

Before surveying, the interns first conducted an analysis of the existing conditions at each site. This provides more information that must be considered when discussing or implementing possible solutions. The descriptions of each site can be found in Appendix D.

4.5.2a Site 1

Site 1 is the slope located on the western side of the island, to the east of the high tide dock. It is 208 feet long, at an angle of 6.0 degrees from south to north. Near the peak of this site, there is an existing channel in the road, shown in Figure 4.8. The hope of this channel is to divert the flow of water towards the coastline to avoid washing away the fill down the hill. However, this is ineffective as more fine material continues to be washed away below it, shown in Figure 4.9, and water remains in the channel without draining to the coast. There is needed maintenance on this culvert to dig out the material it does catch, which is not ideal for island staff.

There is thick vegetation on the coastal (western) side of this site, which mostly protects the road from erosion, besides the area carved by a previous storm. This vegetation includes grasses, bushes, and small trees, as seen in Figure 4.10. The inland side of this site also has similar vegetation and is much thicker.

A point of particular concern at Site 1 is the coastal erosion occurring on the side of the main slope. As shown in Figure 4.11, there is a drainage pipe leading out of the hillside returning water to the ocean area. This pipe is mostly exposed due to coastal erosion from tides and storm surge. This cut out grows with each season, and is beginning to encroach on the road, affecting the ability and general safety of tractor drivers on this road.

Shown in Figures 4.12 and 4.13 are the slope and horizontal profiles, respectively. At maximum, 27 cubic yards of fill would be needed for this site. At minimum, only three cubic yards would be needed to return the roads to a flat surface.

Figure 4.8: Culvert on coastal slope on the western side of the island 6/16/2022

Figure 4.9: Below culvert on coastal slope on western side of island, 6/16/2022

Figure 4.10: Vegetation on coastal side of slope on site 1, 6/16/2022

Figure 4.11: Pipe protruding from hillside at severe coastal erosion site 6/16/2022.

.

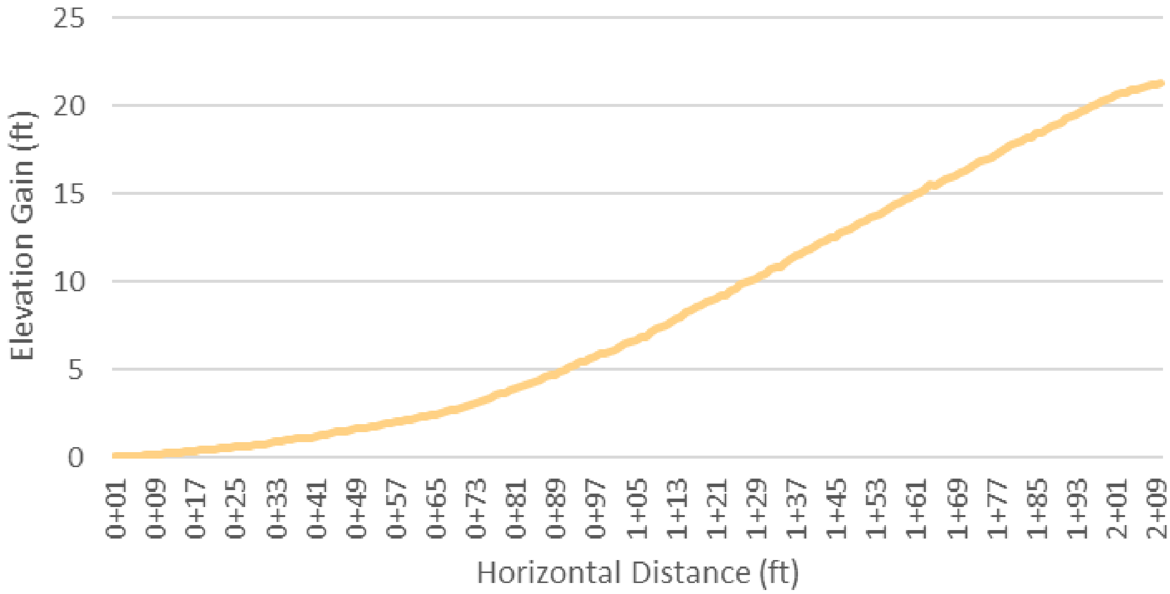

Figure 4.12: Site 1 Slope Profile

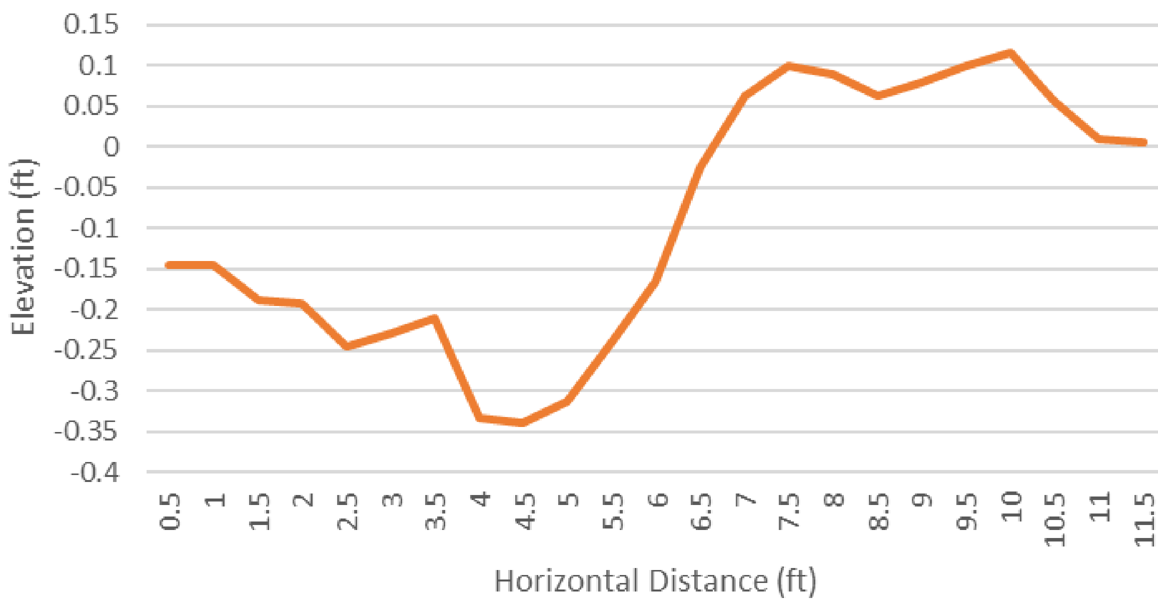

Figure 4.13: Site 1 Horizontal Profile

4.5.2b Site 2

Site 2 consists mostly of the S-turn found outside Laighton Library and includes the downward slope north of the radar tower that takes a left into the S-turn. The slope is 230 feet in length, with a slope angle of about 4.7 degrees facing from southeast to northwest. Fill was recently placed at this site, shown in Figure 4.14. The northern leg of the S-turn has a swale along the southern edge of the road, which flows through a culvert beneath the road. This swale has protected the fine material from diminishing, as shown in Figure 4.15.

The vegetation on either side of the road at this site has the same types of species as in Site 1 and becomes more dense farther from the road. There is also some grass in the center of the road, which would imply that this area suffers from less severe erosion, potentially due to the existing swale. During a brief rain storm, the interns observed the existing natural water path in the road, as shown in Figure 4.16. Once again, this is concerning for the state of the roadway, as the water is flowing through the road itself and is no way diverting into the vegetation on the sides of the road.

Shown in Figures 4.17 and 4.18 are the slope and horizontal profiles, respectively. At maximum, 46 cubic yards of fill would be needed for this site. At minimum, 11 cubic yards would be needed to return the roads to a flat surface.

Figure 4.14: Fill on Site 2, 6/16/2022


Figure 4.15: Swale and under road drainage, preventing the washing away of fines at Site 2, 6/16/2022.

Figure 4.16: Water path during rainstorm, 6/17/2022
at Site 2.

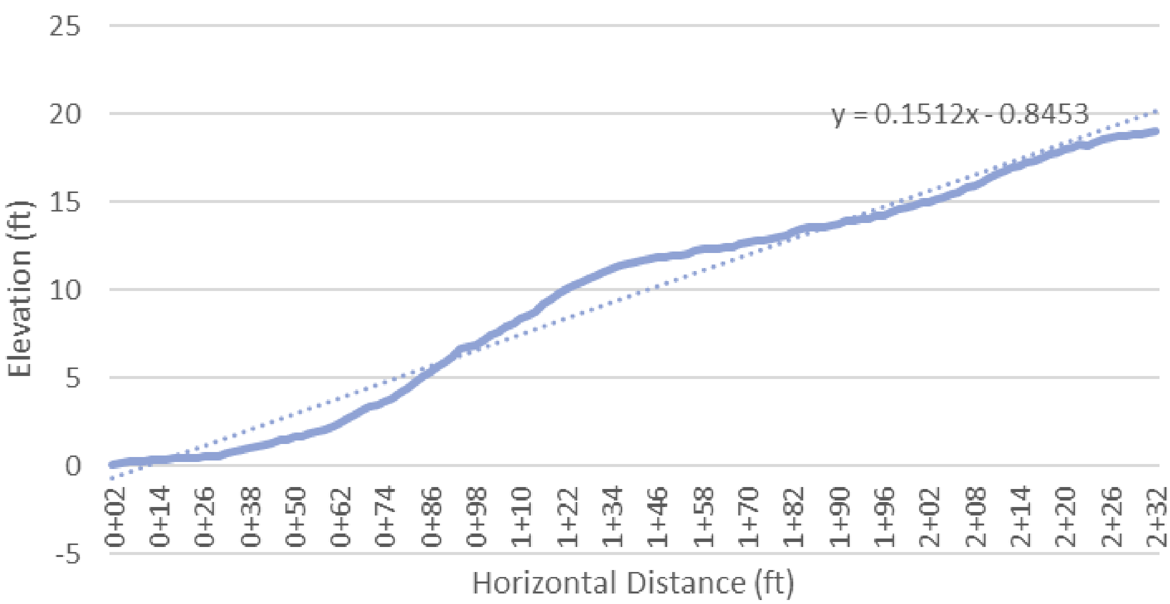

Figure 4.17: Slope Profile Site 2

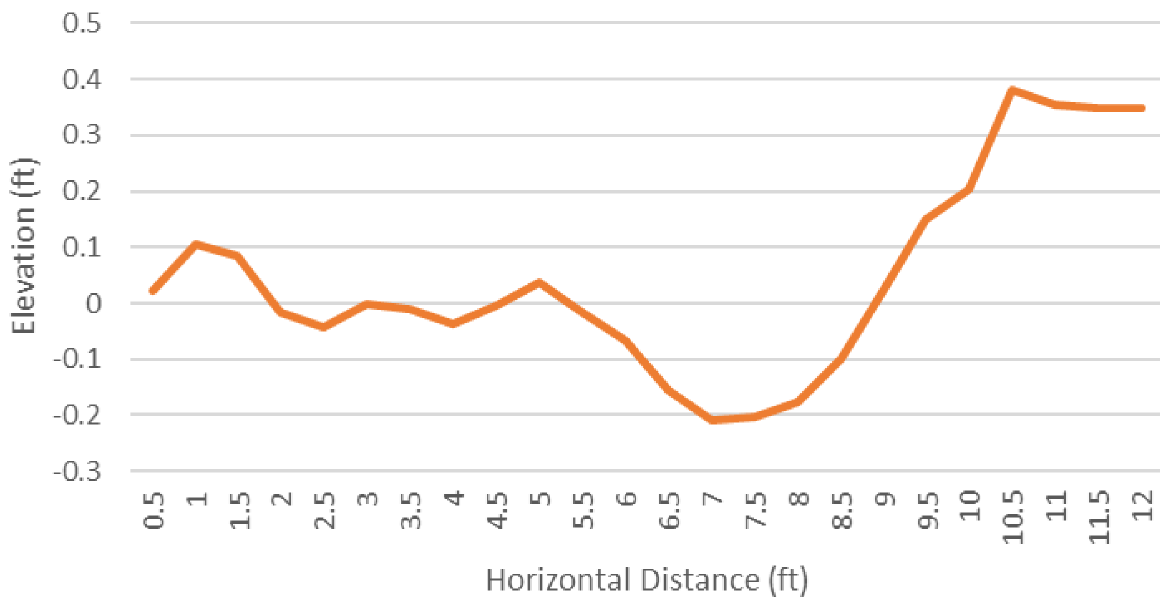

Figure 4.18: Horizontal Profile Site 2

4.5.2c Site 2B

Site 2B is separate from Site 2 because of a very sharp 90 degree turn that splits the slope. The angle of the slope is approximately 4.9 degrees, facing from west to east, and is 81 feet long. The soil of Site 2B is like that of the other sites: dry and dusty, and is defined as type LyC. Fill was recently placed here to fill in the rutting in the road, which is still present where there is no fill. There is ledge present in a few areas of the road's surface, but most notably near the peak of the slope. The vegetation appears to be encroaching on the road itself, more thick on the northern side of the road and bushy on the southern side. The material of the road is consistently on the more fine side with larger gravel at the road's edges where there is rutting.

Shown in Figures 4.19 and 4.20 are the slope and horizontal profiles, respectively. At maximum, 11 cubic yards of fill would be needed for this site. At minimum, only five cubic yards would be needed to return the roads to a flat surface.

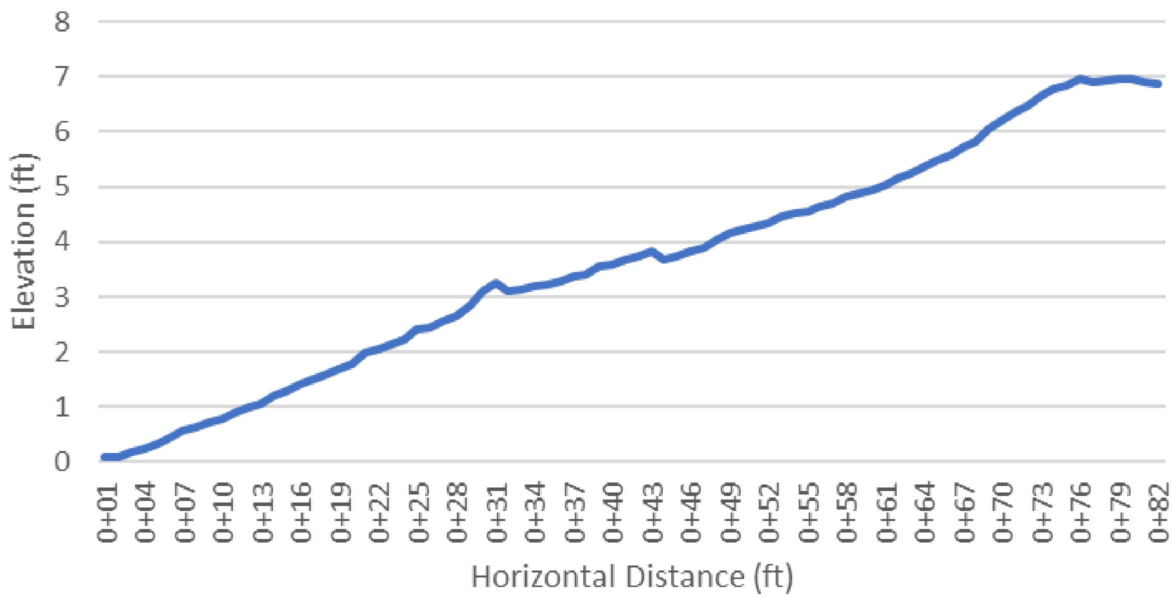

Figure 4.19: Slope Profile Site 2b

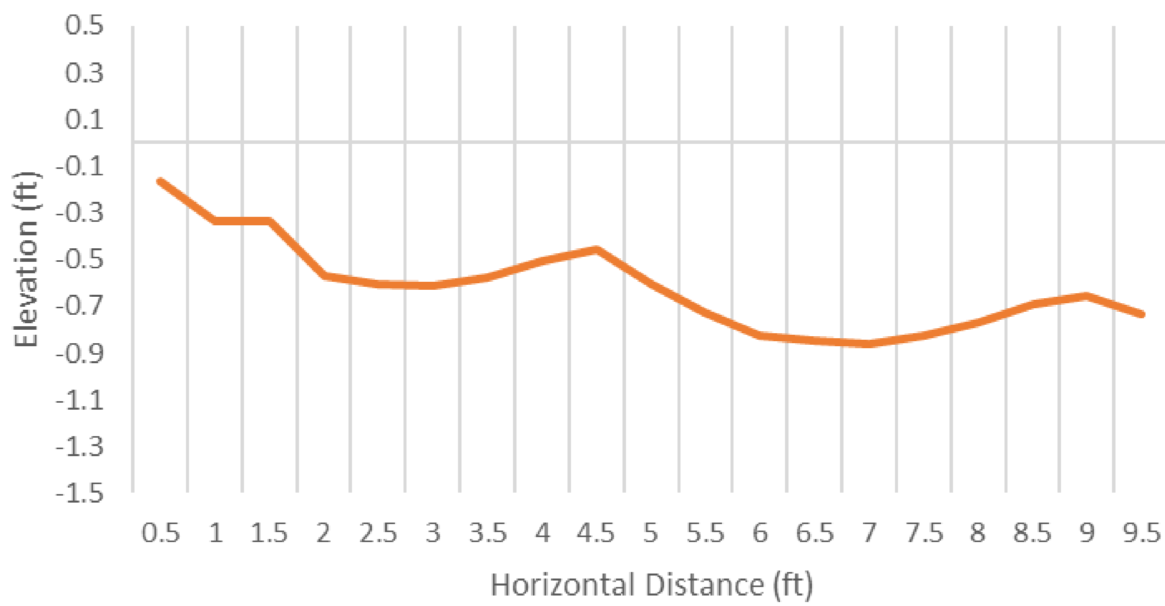

Figure 4.20: Horizontal Profile Site 2B

4.5.2d Site 3

Site 3 includes a long slope beginning near Kingsbury and the radar tower and travels all the way down to the SML dock. The total length of this slope is 345 feet, with a slope of about 5.1 degrees facing from east to southwest. This area is of concern, as the rutting caused by erosion has made a kind of natural swale existing within the roadway on the right hand side when looking down the slope. The road itself seems to be slanted down across the width of the slope, encouraging the formation of this natural swale (Figure 4.21). There are many cases of exposed ledge present in the road as seen in this figure, which could pose issues for installation of culverts.

Soil quality appears dry and powdery in most places, if not just ledge breaking through the ground surface. Rock coverage includes loose gravel varying in size. Vegetation appears sparse in the road, with occasional strips down the middle of the road, and abundant grasses and shrubs lining the edges. Some larger rocks are present in the surrounding vegetation as well.

Shown in Figures 4.22 and 4.23 are the slope and horizontal profiles, respectively. At maximum, 98 cubic yards of fill would be needed for this site. At minimum, 19 cubic yards would be needed to return the roads to a flat surface.

Figure 4.21: The natural swale in the roadway seen on 6/16/2022 and during the rainstorm 6/17/2022. Water flows through the roadway, deepening the swale and increasing the removal of fines.

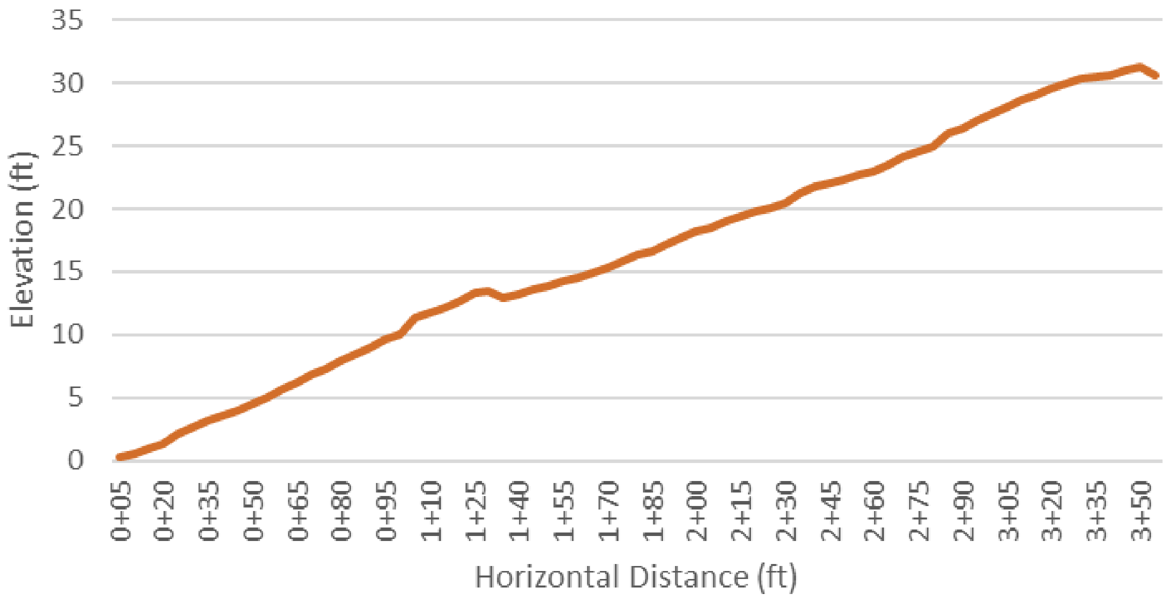

Figure 4.22: Slope Profile Site 3

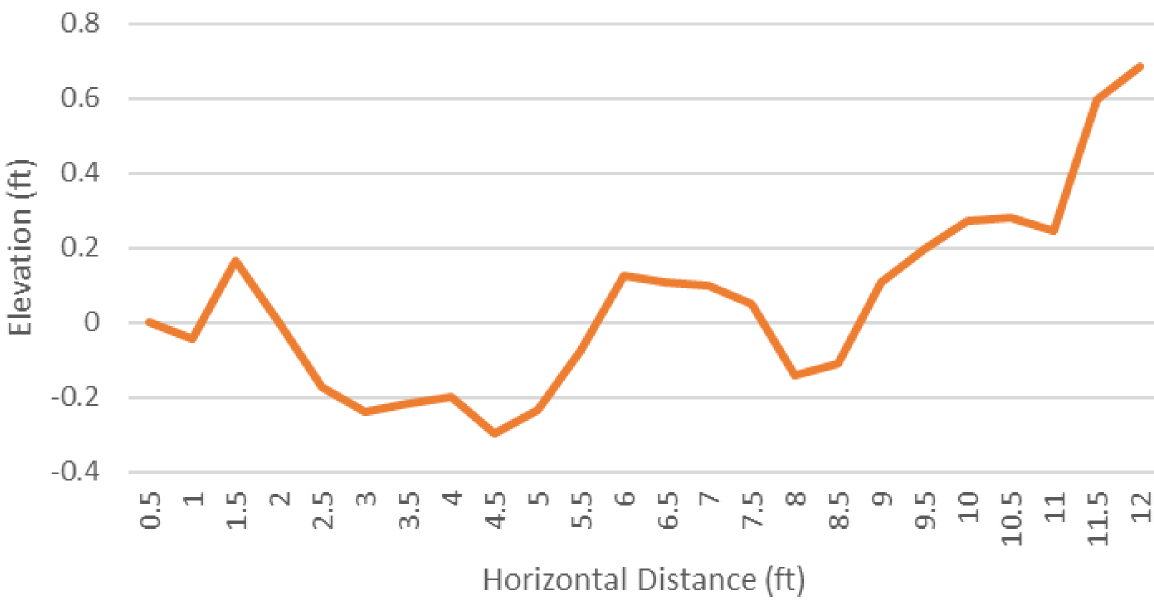

Figure 4.23: Horizontal Profile Site 3

4.5.2e Site 4

Site 4 is the longest and most shallow site surveyed at 378 feet long. The angle of this slope is 1.7 degrees north of the peak (facing from southwest to northeast) and is about 3.2 degrees south of the peak (facing from northeast to southwest). Site 4 is along the same roadway as Site 1, also along the northwestern side of the island.

Ledge frequently surfaces along this slope, but is most evident at the top and bottom of the slope. There is more fine material towards the slope's peak, with more gravel-like material towards the lower ends. There are minimal effects of erosion that become more severe where the slope approaches Site 1. There is light, grass-like vegetation on the north side of the road with very dense vegetation along the southern side. Lastly, on the side of the slope closer to Site 1, there appears to be some geotextile material that should either be replaced or removed to be an efficient method of retaining the finer material.

Shown in Figures 4.24 and 4.25 are the slope and horizontal profiles, respectively. At maximum, 62 cubic yards of fill would be needed for this site. At minimum, 14 cubic yards would be needed to return the roads to a flat surface.

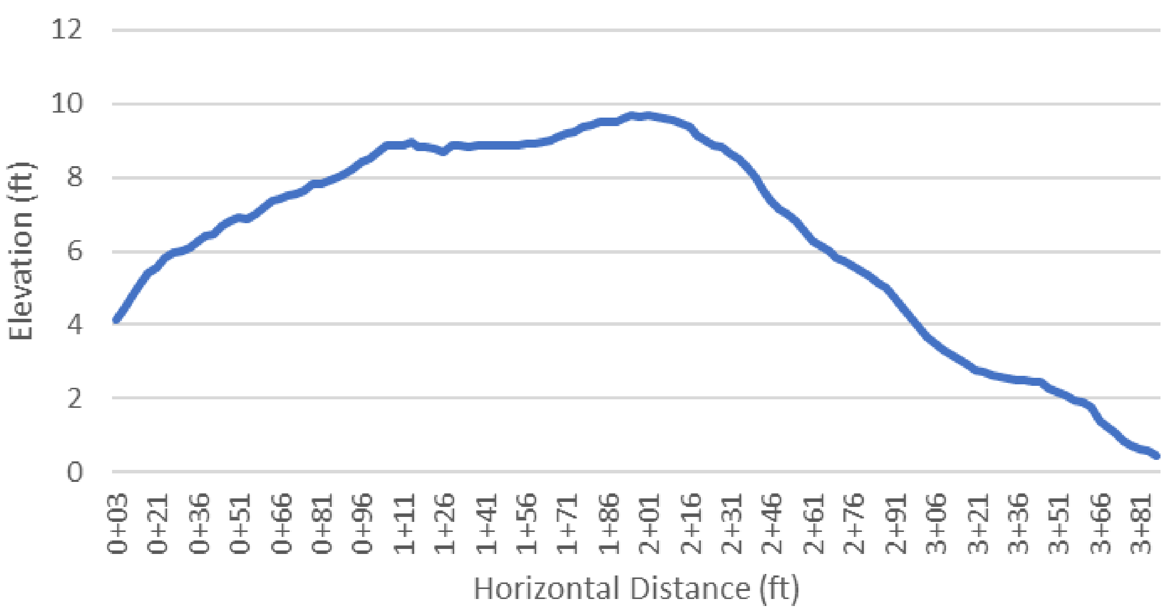

Figure 4.24: Slope Profile Site 4

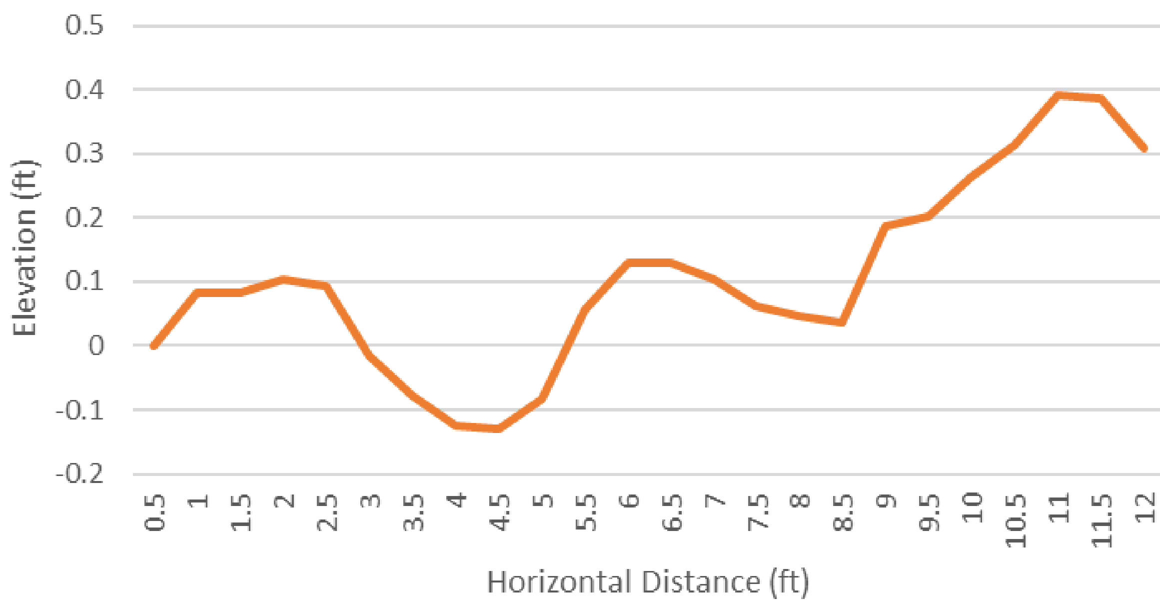

Figure 4.25: Horizontal Profile site 4

4.6 Conclusions and Recommendations

Erosion is a large problem on Appledore, and many island functions rely on continued road maintenance and upkeep. The interns recognize that these roads are often in use by island staff and students alike, as well as touring visitors. The heavy foot and vehicle traffic as well as harsh weather conditions in the offseason requires a durable erosion solution. Realistically, any proposed solution will require some degree of maintenance by island staff for optimal function. Each site must be evaluated differently, and a variety of techniques should be used for each site. If all the sites are to be filled in the proposed "crown" fashion, a total maximum of 500 cubic yards would be needed, while a minimum of 250 cubic yards would be needed to fill in the existing rutting. The usual vendor that SML gets its fill from, LPA, has been unable to be contacted. According to an online source, Home Guide, gravel costs between $25-62 per cubic yard. At $62 per cubic yard, a maximum of $31,000 would be needed for "crown" profiles, and at $25 per cubic yard, $12,500 wouldbe needed. Similarly, to fix the present rutting, at $62 per cubic yard, $15,500 would be needed, or $6,250 would be needed at $25 per cubic yard (HomeGuide).

4.6.1a Site 1 Solutions

Since there is the aforementioned area of severe erosion, the interns believe that the road must be shifted inland by approximately two feet, which would involve cutting and removing some of the thick vegetation. In addition, because this site is closest to the coast and most vulnerable to coastal erosion, a soft or hard scape retaining wall is recommended. However, it must be noted that there is a pipe outfall that discharges on the coastal side, also shown in Figure 4.11, which must be considered when designing or constructing a retaining wall.

Additional channels down the slope may be necessary, as well as upgrading or replacing the existing channel. This channel could be more successful if it were on a more inclined slope towards the coast, allowing for more water flow. Additional culverts could be made of a material similar to highway guardrails. These guardrails would be wider, but would have more of a slope gradient than the existing culvert, so vehicles are still able to drive over them. The use of W-Beam highway guardrails invites a sustainable solution that allows for existing materials to be repurposed. W-Beams are used in outdoor environments with a range of weather situations, and are known for general durability and strength. The use of tractors and trailers over these W-Beam culvert installments would cause virtually no damage, and they would last for an extended period of time even in the coastal environment due to their general sturdiness. Twelve-foot recycled guardrails are available at CWS Fence and Guardrail in Andover, NH for a cost of $40 each, and the rails can be picked up by island staff.

4.6.1b Site 2 & 2B Solutions

At the northern side of the most dramatic bend of Site 2, there is a steep slope of grass that could serve as an area of drainage if care is taken to avoid draining into the road of Site 1. Another potential drainage area could be between the road and the library. It is at a higher elevation than the bend, but it may be challenging to add drainage due to the close proximity of the library.

Retaining the drainage area at the bend and adding highway guardrail channels across the road sloping towards the northeast would allow for water to drain off the road and would not add additional erosion potential for Site 1.

Similarly, adding guardrail channels facing the northeast and enhancing the efficiency of the existing swale without the drainage area could be another potential solution. Adding a channel at Site 2B would also be advised, though facing northwest instead of northeast. There is very thick vegetation between Site 2B and Site 4, so there is minimal risk of creating a flooding problem for Site 4. Any mitigation of flow that occurs at Site 2B would also protect Site 2 from erosion. The interns propose either using a guardrail system, or filling in the roads with a “crown” shape with drainage areas on either side of the road.

4.6.1c Site 3 Solutions

Off of both sides of the road, there appears to be a shallow ditch or general elevation decline that could be fashioned into a swale or drainage area, allowing for an alternate path for flowing water Figure 4.27. Interns suggest that swales be installed along both sides of the road and using the “crown” profile shape, or using swales as well as level spreaders in the road itself, encouraging water runoff so as to avoid washing away fines and gravel making up the road. A swale on both sides of the road would discourage water from entering the road from the uphill side as well as encouraging water already on the road to run off on the downhill side. Level spreaders, partly shown in Figure 26, would slow the water's movement down the road, allowing for as much of the existing road to be preserved as possible while still allowing through traffic.

Another option includes installing channels, as discussed for Site 1. While this would prove effective in the case of this slope, there could be issues in the installation process due to the presence of exposed ledge. The depth at this location is shallow, and varies from shallow to no depth throughout the site. Channels may be installed in certain areas; however, it may not be feasible for the entire slope.

Figure 4.26: Ledge enhanced as natural level spreader; dig in front to create more of a ledge, implement riprap on side to help drainage into surrounding vegetation.

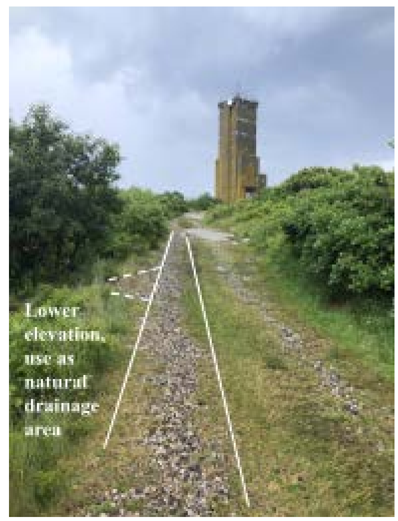

Figure 4.27: Potential drainage area to divert water flow from roadway to manmade swale offroad.

4.6.1d Site 4 Solutions

Site 4 appears to be the least affected by stormwater erosion. However, the interns have noticed that the staff drive fast along this stretch of road, which would contribute to loss of fine material. As a result, the interns propose adding two or three level spreaders down the slope, which would serve a dual purpose: to slow down the flow that will increase its velocity down the long slope, and also to act as speed bumps for the island staff to drive slower.

An additional solution would be to add one to two culverts down this slope that could drain onto the western side of the road, which is closest to the coast. Either of these solutions would be instead of a filled "crown" profile with swales on either side of the roads.

4.6.2 Future Projects

A future project idea could be to investigate types of fill that could be used for the roads. This investigation could consist of the least expensive, most environmentally friendly, and the most effective types of fill. One potential idea was to mix some asphalt-type material already present on the island with gravel fill in hopes that the gravel would be able to compact and adhere better to itself.

Another idea for a future project could be thinking of ways to filter the water out of the proposed highway guardrail channels, leaving the fines and gravel either in the channel or, ideally, in the road.

4.7 References

Birchler, Justin J. "National Assessment of Hurricane-Induced Coastal Erosion Hazards ." *USGS*, 2014, https://pubs.usgs.gov/of/2014/1243/pdf/ofr2014-1243.pdf.

"How Much Does Crushed Stone or Gravel Cost?" *HomeGuide*, https://homeguide.com/costs/gravel-prices

5 Rainwater Collection for Celia Thaxter's Garden

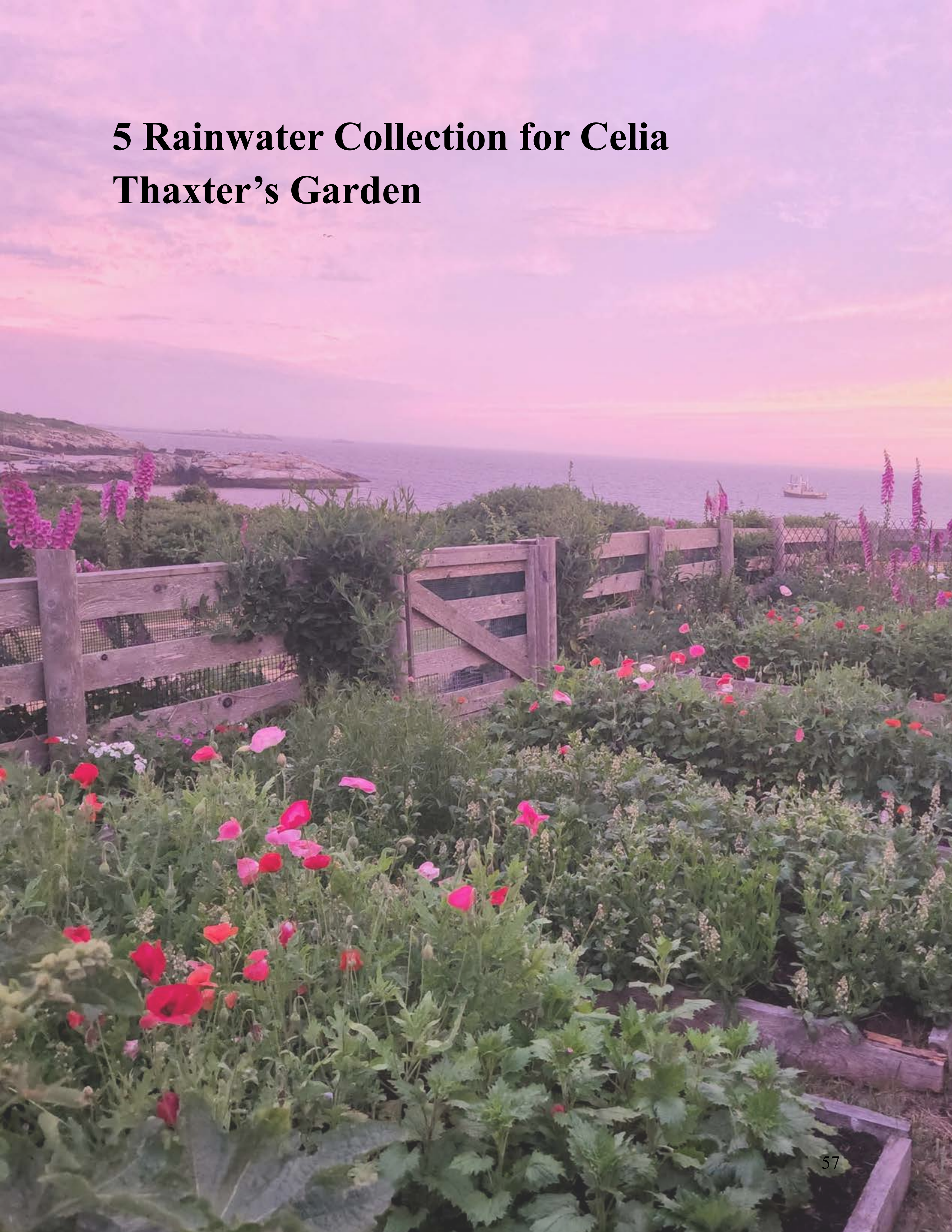

Lead Interns: Tess Hays and Jason Shao

5.1 Background

The Celia Thaxter garden is an important historical aspect of Appledore Island. Tourists come from across the country to view the flowers expertly kept with incredible likeness to Thaxter's original garden through the hard work of the Garden Steward, Terry Cook. It is important to maintain ideal growth conditions for the flowers throughout the season so the garden must be watered daily with the current drip irrigation system. The primary source of water for this system are two 800 gallon tanks that collect rainwater through a gutter on the roof of the Utilities Building. The water is then pumped from these tanks to the garden's drip irrigation system which then waters the flower beds. The current storage tanks are depleted after about 9 days, assuming no additional water is collected and 173 gallons a day are used (SEI Report 2016). The Shoals Marine Lab wishes to have the garden's water sourced solely from collected rainwater. In the case of a drought or general lack of rain, increased storage and collection methods are desired that can be looped into the current system with minimal difficulty or rearranging.

5.1.1 Current Rainwater Collection System

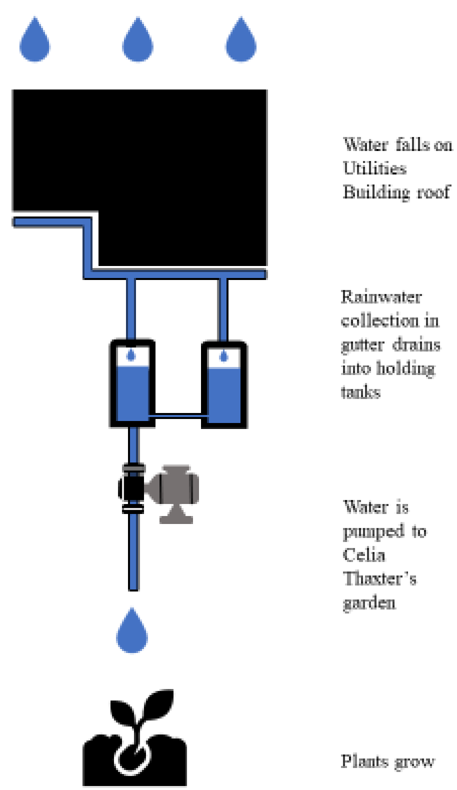

Figure 5.1: Current Rainwater Collection System

5.1.2 Rainfall Data Appledore Island

Table 5.1: Rainfall Data Appledore Island 2020-2022

Year	Month	in Rainfall
2022	April	2.35
	May	1.08
	June	2.08
	July	-----
	August	-----
	Total	**5.51**
2021	April	-----
	May	2.84
	June	1.67
	July	8.45
	August	3.43
	Total	**16.39**
2020	April	1.11
	May	1.34
	June	2.09
	July	2.85
	August	0.85
	Total	**8.24**
2019	August	2.82
	Total	**2.82**
2018	NO DATA	-----
2017	NO DATA	-----

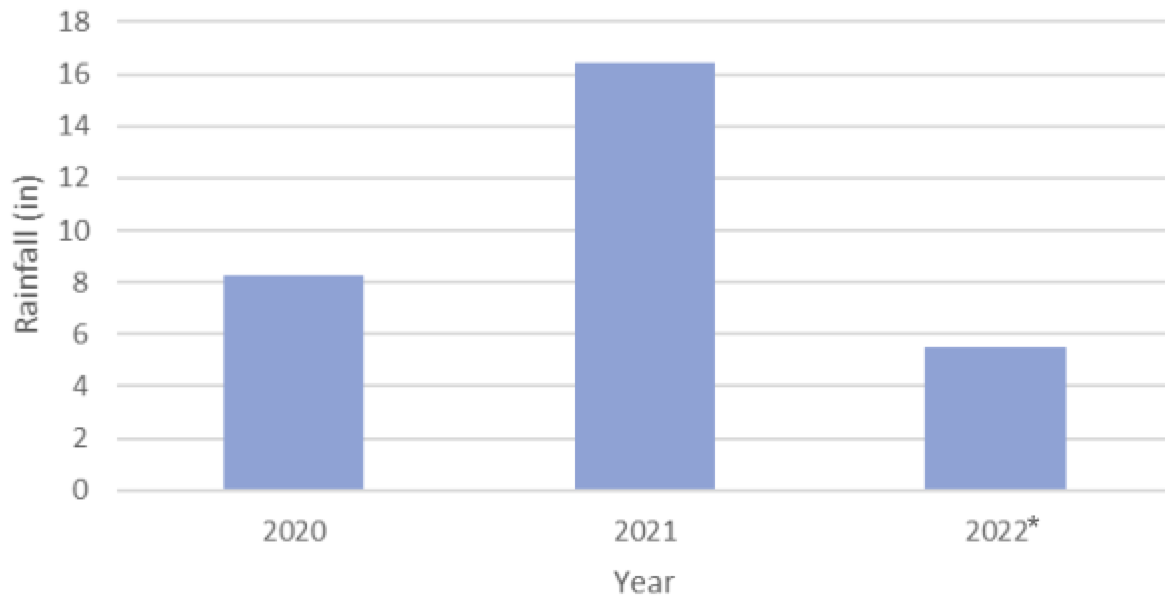

Figure 5.2: Yearly Rainfall (in) April-August, *Year still in progress

More rainfall data will continue to be collected in upcoming years, and a reassessment of proposed solutions could be conducted in five to ten years time. A lack of data available to the interns has impacted suggestions, and a better understanding of rainfall patterns on Appledore Island could be the deciding factor between two proposed solutions. The only available rainfall data are shown in Figure 5.2, and data were taken from downloading CSV files (Sustainable SML, Precipitation).

5.2 Purpose

The purpose of this assignment is to improve the current gutter system for rainwater collection in the 800 gallon tanks located at the base of the Utilities Building roof, as well as draw plans for increased water storage using more tanks. The tanks cannot be installed near the existing tanks due to lack of ground space and ledge preventing digging. This increased water storage would allow for the garden to be watered solely from rainwater, allowing water from the island freshwater system to fulfill other island freshwater demands, lessening strain on the system and decreasing the number of times the reverse osmosis machine needs to be run to meet the freshwater demand.

5.3 Scope

The interns will observe rainwater behavior with the current gutter, and provide suggestions for an improved gutter system so as to increase the efficiency of the water collection into existing tanks. Additionally, interns will propose the size and location for tank installation for increased water storage, as well as how these tanks will be incorporated into the existing system with minimal to no changes to how the system functions.

5.4 Methods

5.4.1 Ideas for New Storage

Option 1: Pole Barn Storage

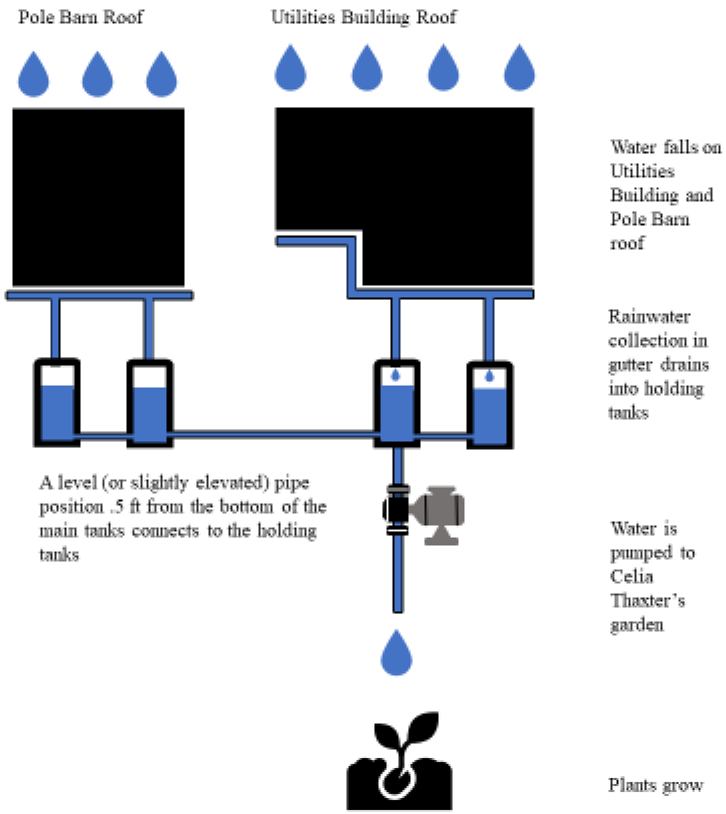

Figure 5.3: Proposed storage additions behind Pole Barn, Option 1

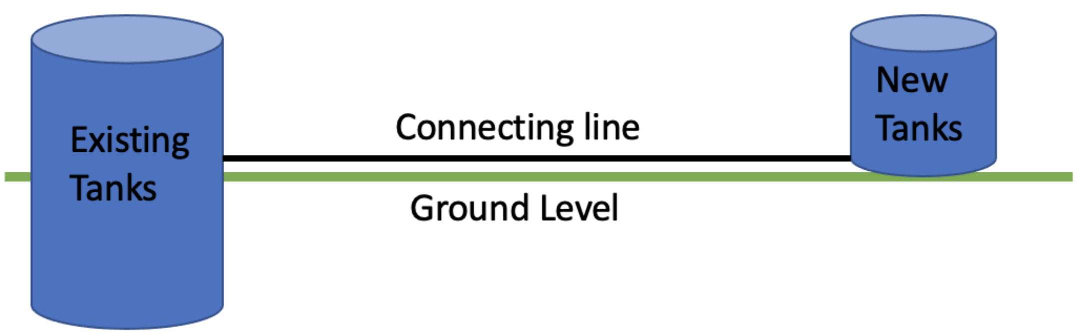

Figure 5.4: New tanks would be installed above ground. The connecting line would be at the bottom of the new tanks. The line in the existing tanks would be connected above ground where the tank is exposed. The existing tanks would be filled up to the ground level. After the tank reaches this point, both tanks will fill. Then as water is needed, it will be pumped from the bottom of the existing tanks from a submersible pump, emptying both tanks.

Option 1 proposed by the interns requires the installation of a multitude of tanks behind the Pole Barn roof. Another gutter system could be installed for this roof, allowing the additional tanks to collect and store roof water. These tanks would be linked together and connected to the existing tanks through a level or slightly tilted pipe. Since the elevation between the existing storage tanks and the proposed new location seems relatively constant, if the tanks are connected at the bottom then the water levels of the tanks should even out. This would eliminate the need for an additional pump in the system. Water for irrigation would continue to be pumped through the existing system, and general piping and system functions would remain unchanged, only the storage capacity would increase. This would allow minimal disruption to the garden watering system, which would be ideal during the growing season (the summer) when this installation would occur.

Option 2: Garden Hill Storage:

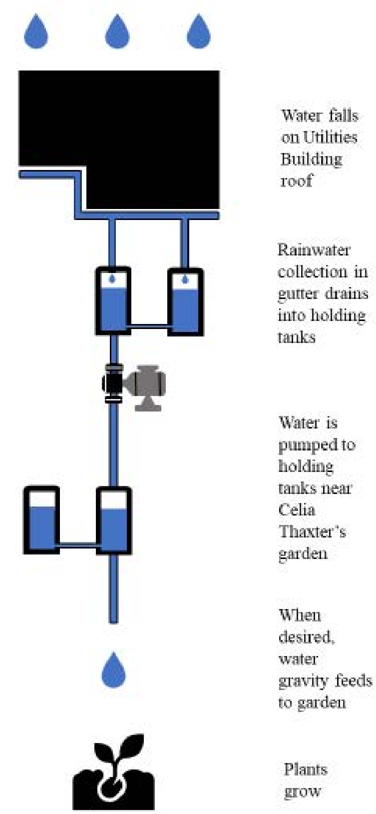

Figure 5.5: Proposed storage additions behind vegetation on hill near Celia Thaxter Garden, Option 2

Option 2 was proposed by Ross Hansen. In this scenario, additional tanks would be located up the hill closer to the garden. This part of the system would work similarly to how the RO is run. When there is excess green energy, water from the existing tanks would be pumped up the hill to the new storage tanks. Water in this new storage would then flow to the garden as needed through gravity feeding when the system is turned on/a valve is opened. The tank would be incorporated into the current system in the least invasive way possible, where one of the existing above ground lines would be cut and run up to the storage tank location. Because dramatic changes to the current watering system would not be needed, installation would have minimal effects on the garden watering, and the transition between systems would be smooth.

5.4.2 Data Acquisition

Figure 5.6: Rainwater overflow at Utilities Building gutter, leading to current rainwater storage tanks

Figure 5.7: Utilities Building gutter during rainstorm; note the water dripping between the edge of the roof and the building

Interns examined the gutter performance during a rainstorm. Common complaints were that the gutters overflow during heavy rain or that much of the roof runoff shoots over the gutter. These aspects were focused on during observation of the gutter performance. Interns also remeasured the Utility Shed roof area that should be collecting rainwater by using a measuring tape. Estimations were also done using Google Maps to confirm this measurement. For additional rainwater collection, interns measured the approximate surface area of the Pole Barn, and found it to have approximately 697 ft^2 lateral area for rainfall. Interns looked at data available for typical rainfall for the summer months (April to August) in which the garden needed to be watered to approximate the volume of rainfall in order to properly size storage tanks. Interns also surveyed the relevant elevations for both potential options using a transit and rod. The goal of this was to quantify the elevation gain so that the necessary heights to place tanks could be determined.

5.4.3 Garden Needs

The 2016 SEI group, while assessing the efficiency of the new garden drip irrigation system, found that about 170 gallons of water were used per day. Talking to Terry Cook, it was determined that levels of pH, nitrate, and ammonia should not be a concern for the plants.

5.4.4 Calculating Volume of Rain

$$Inches\ of\ Rainfall * Square\ Footage\ of\ Roof * \frac{144\ in^2}{1\ ft^2} = Potential\ Volume\ of\ Collected\ Rainwater$$

5.4.5 Change in Volume of Tanks

$$\Delta V = Tank\ Cross\text{-}Sectional\ Area * (\Delta Tank\ Level_{left} + \Delta Tank\ Level_{right})$$
$$\Delta Tank\ Level = Tank\ Level_{initial} - Tank\ Level_{final}$$

5.4.6 Gutter Efficiency

$$Gutter\ Efficiency = \frac{Actual\ Volume\ of\ Collected\ Rainwater}{Potential\ Volume\ of\ Collected\ Rainwater}$$

5.4.7 Height Requirement of Proposed Storage Tanks - Option 2

In order for Option 2 to function, the new tanks must be able to gravity feed to the garden distribution system. Tables from the 2015 SEI report show that the minimum pressure at the garden must be 25 psi, the velocity of flow to the garden is 3.32 ft/s, and the velocity at the garden is 1.88 ft/s. Knowing the elevation of the hill as well, the interns can use Bernouli's equation to determine the height the new tanks need to be to overcome the 25 psi minimum.

$$\text{Bernoulli's Equation: } \frac{P_{in}}{\gamma} + \frac{V_{in}^2}{2g} + z_{in} = \frac{P_{out}}{\gamma} + \frac{V_{out}^2}{2g} + z_{out}$$

5.5 Results and Analysis

5.5.1 Elevation Surveys

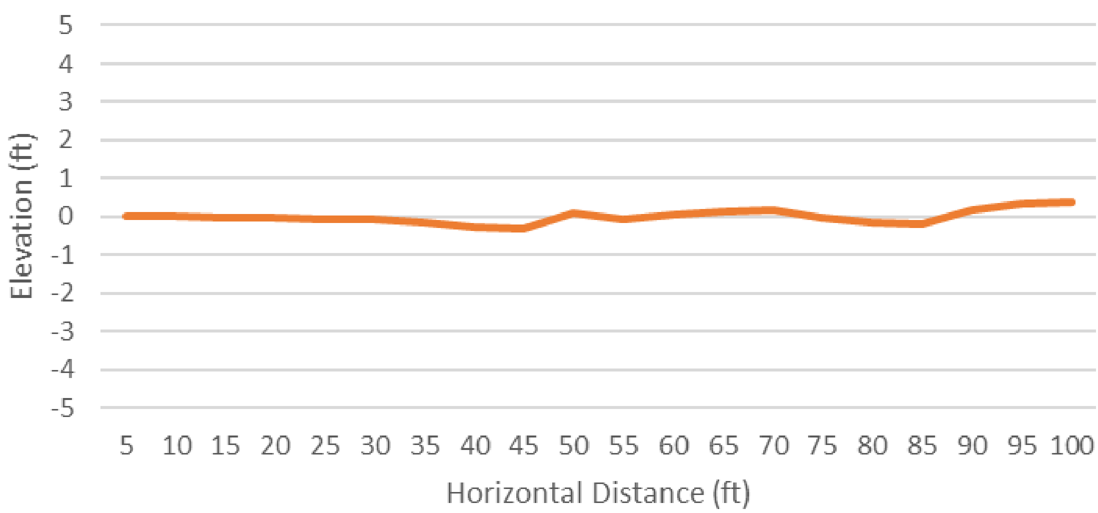

Figure 5.8: Elevation survey between current storage tanks and proposed location (Pole Barn)

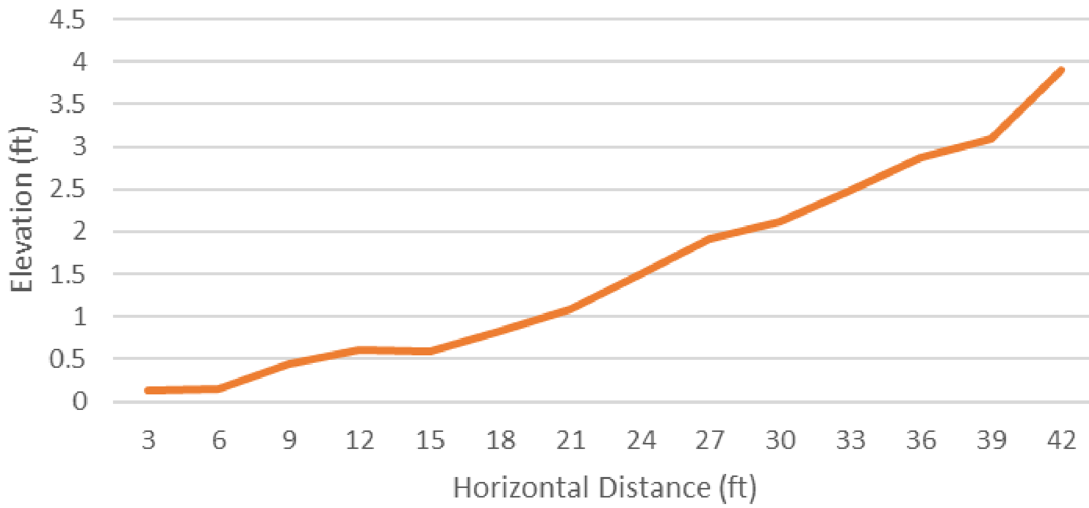

Figure 5.9: Elevation survey between irrigation control panel (Celia Thaxter Garden) and Option 2 proposed location.

The survey confirmed that for the proposed location of Option 1, there is a net elevation gain of approximately 0.35 feet, or about 4.25 inches between existing tanks and the area behind the Pole Barn. As stated previously, this lack of elevation would work well to connect tanks that would equalize without the use of a pump. From the current garden water distribution system to the location Ross proposes up the hill, there is about a four foot elevation gain. For this option, elevation gain is preferred, since there needs to be elevation for the water to flow down to the garden.

5.5.2 Height Requirement of Proposed Storage Tanks - Option 2

Minimum pressure at the garden - 25 psi (SEI Report 2015):

$$P_{out} = 25\,psi = 172369\,Pa$$

Assume 6 in (.1534 m) water always present, so water pressure in the tank (minimum) is:

$$P_{in} = P_{atm} + \rho g h = 101325\,Pa + 1000\frac{kg}{m^3} * 9.81\frac{m}{s^2} * .1524\,m = 102820\,Pa$$

The height elevation the bottom of the new tanks needs to be above the garden:

$$\frac{102820\,Pa}{9.81*10^3\frac{N}{m^3}} + \frac{(1.012\frac{m}{s})^2}{2*9.81\frac{m}{s^2}} + z_{in} = \frac{172369\,Pa}{9.81*10^3\frac{N}{m^3}} + \frac{(.573\frac{m}{s})^2}{2*9.81\frac{m}{s^2}} + 0m \Rightarrow z_{in} = 7.05m \approx 23\,ft$$

The interns calculated the approximate height needed to achieve gravity feeding from the storage tanks to the garden. Using Bernoulli's equation for fluid flow, the interns found a total elevation difference of about 23 feet was required to obtain a water pressure entering the garden of about 25 psi, which was the minimum pressure required for full water circulation throughout the garden. This calculation was made assuming the lowest water level in the tank was six inches, or half a foot, as stated by previous interns in SEI Report 2015. The land elevation difference acquired through surveying was approximately four feet, so an added tank elevation of 19 feet would be required for gravity feeding to be possible.

5.5.3 Available Tanks

The current tanks in the system have a capacity of 1,600 gallons of water. According to SEI Report 2016, the drip irrigation system uses 173 gallons of freshwater a day. Assuming the freshwater storage tanks begin at full capacity, the garden could be watered solely from the storage tanks for about nine days before the tanks are drained. After this time, freshwater would have to come from the well/drinking water system. Many of the summer months experience droughts or minimal rainfall (see Table 1), so doubling or tripling this storage capacity would be ideal.

Details for tanks already in SML's possession were provided for the interns, and the benefits and drawbacks for each available tank were taken into consideration, see Table 5.2 for tank details.

Table 5.2: Tank Characteristics

Tank Type	Description	Volume, ft^3	Gallons	Number of tanks
Type 1	cylinder, d8'	192.7093	1441.566	3
Type 2	cylinder, d9'	190.8765	1427.855	4
Type 3	square base, 6'x6'	120	897.6624	5
Type 4	rectangular base, 52"x30"	13.54167	101.2987	2

The interns ultimately decided that lofting a tank 19 feet in the air would be impractical for maintenance, aesthetics, and cost, so Option 1 (installation behind the Pole Barn) was used as the criteria for evaluating tank options.

Prior to the installation of any tanks, the area behind the Pole Barn must be cleared of some of the vegetation present. There are two pipes: an old steel pipe from the hotel era, and a ribbed drainage pipe. Upon consultation with island engineers and directors, it was found that the hotel pipe is no longer in use, and can be removed from the site. The ribbed pipe has little to no drainage output, and can also be removed or relocated. Caution should be taken when excavating the area for the presence of ledge, as the depth of the soil is unknown. The tanks must also be level or slightly above the current tanks collecting roof runoff from the Utilities Building, to ensure the level of water remains the same in both groups of tanks. Ideally, the pipe attaching the tanks would be installed half a foot from the base of the tank, ensuring the tanks never fully drain of water (this concept is followed for the current tanks as well).

Options for installation include the installation of all three Type 1 tanks (cylinder with diameter of eight feet). The width of the Pole Barn roof is about 41 feet, so all three tanks could easily fit behind the building with room between for maintenance and general maneuverability. These tanks would add approximately 4,300 gallons of water storage, almost tripling the current storage capacity. Assuming all storage tanks are filled, the tanks would take 34 days to drain assuming no replenishment of water. In the past three years, some type of precipitation has been measured for each month (see Table 1). This storage capacity for the tanks would greatly benefit the island in the dryer months, especially if the tanks are in full operation during the months of April and May.

Another option is the installation of three or four tanks of Type 2 (cylinder with diameter of nine feet). Type 1 and Type 2 have similar volumetric capacities, however there are more tanks available for Type 2 (3 tanks for Type 1, 4 for Type 2). Installing three tanks of Type 2 would be about the same volumetric gain as installing three of Type 1. Installing four tanks of Type 2 would bring overall potential water storage up to about 7,300 gallons, and assuming no water replenishment the tanks would be able to water the garden purely from roof runoff for 42 days (assuming 173 gallons needed daily).

There are five available Type 3 tanks. Installing all five tanks may be spatially tight behind the building, but this would add 4,500 gallons of water storage to the current 1,600 gallon system, increasing total storage capacity to 6,100 gallons of storage. Assuming all tanks are full, the system could water the garden for about 35 days before running out of water. Installing just four of these tanks would allow for more space for maintenance and upkeep of the tanks. This would still increase storage potential to 5,200 gallons, which would last for about 30 days before depletion.

While these tanks are already in possession of SML, they are not present on the island. The greatest costs to SML would be the transportation of the tanks to Appledore. Upon reaching the island, the tanks would have to be moved throughout the road system to reach the Pole Barn. The excavation process should not be too costly, as machines for this are on the island (assuming island engineers would carry out the installation).

5.5.4 Gutter Efficiency

Documentation of the gutter showed that during light rain, much of the roof runoff dripped between the roof and the gutter itself, falling short of landing in the gutter. During heavy rain storms, the gutters would overflow and much of the roof runoff shoots over the gutter, again missing the means for water collections in the tanks. It was also observed that the left side corner near the tanks overflows while the right side past the drainage pipe pools up without being collected.

$$Potential\ Volume\ of\ Collected\ Rainfall = (.11in)(1800ft^2)(\frac{144\ in^2}{1 ft^2}) = 28512\ in^3$$

Table 5.3: Sample Calculations Potential Volume of Collected Rainfall, 06/27/2022

Pre-Storm		**Post-Storm**	
Water Level from top (in)		Water Level from top (in)	
Left Tank	Right Tank	Left Tank	Right Tank
10.51	10.00	8.23	8.82

$$Tank\ Radius = 33\ in$$
$$Tank\ Cross\text{-}Sectional\ Area = \pi r^2 = \pi * (33\ in)^2 = 3421\ in^2$$
$$\Delta V = 3421\ in^2 * ((10.51\ in - 8.23\ in) + (10.00\ in - 8.82\ in)) = 11837\ in^3$$

$$Gutter\ Efficiency = \frac{11837\ in^3}{28512\ in^3} = .42 = 42\%$$

Table 5.4: Gutter Efficiency Calculations, 06/27/2022

Rain (in)	**Usable Rain (in^3)**	**Total ΔV (in^3)**	**Efficiency**
0.11	28512	11853	0.42

Table 5.5: Gutter Efficiency Calculations, 07/01/2022 - 07/02/2022

Rain (in)	**Usable Rain (in^3)**	**Total ΔV (in^3)**	**Efficiency**
0.03	7776	2424	0.31

Table 5.6: Gutter Efficiency Calculations, 07/05/2022-07/06/2022

Rain (in)	**Usable Rain (in^3)**	**Total ΔV (in^3)**	**Efficiency**
0.65	168480	70562.1345	.42

5.6 Conclusions and Recommendations

5.6.1 Improving the Gutter

It is evident from documentation and comparing the actual rainwater collection to the full potential collection that the gutter system is not performing very well. As shown in Tables 5.4, 5.6, and 5.7, the gutter system only functions with 30-40% efficiency. In order to capture more of the available rainwater, a few things can be changed about the gutter system. First, increasing the gutter size from four inches to six inches would help prevent water overflowing the gutters or missing them completely. Additionally, ensuring the gutters are flush to the wall will help prevent water from flowing between the wall and the gutter.

5.6.2 New Storage

The interns recommend Option 1, which entails putting new storage tanks behind the Pole Barn. Reference Figures 5.3 and 5.4 in Section 5.4.1. The addition of these tanks in this location would be unobtrusive to the rest of the system. Additionally, the elevation gain between the Pole Barn and the existing tanks is very low. The new tanks could be installed above ground and be connected to the existing tanks where they are exposed above ground. Then the water levels in them should equal out without the need of a pump. As a consequence, the current submersible pump can continue to be used to transport water from the tanks to the garden.

Looking at Type 2, this type of tank holds about 190 gallons of water at a time and is three feet tall. The existing tanks at the edge of the Utilities Building roof protrude about three feet above ground, with the bottom half buried underground. The new tanks have bulkheads on the bottom, allowing for drainage or pipe connection. The interns recommend that four Type 2 tanks are installed above ground, elevated just enough so the bottom of the tank can be accessed. The bulkheads should then be fitted with a similar type of piping that has been used in the system already (the black piping that runs the water up to the garden). The piping should be attached so that it can be removed, similar to the way where the hose to the garden can switch between the well and the rainwater tanks. This would allow for easy drainage in preparation for the winter months. This piping would then run above ground to the existing tanks, where a hole could be drilled into the side. The piping could run through this hole and allow water to flow into these tanks. For a tank installation visual, see Figure 5.4 (Section 5.4.1) With this configuration, the existing tanks would fill up about halfway before reaching the level of the new connection. Then once this level is reached, the new tanks and the existing tanks would fill equally. This would result in no modifications to the current pumping system, and allow for relatively easy installation. For increased water collection, a gutter system could be installed on the Pole Barn roof, allowing for additional water drainage to the newly installed tanks, increasing the overall amount of rainwater potentially available for garden use.

If running the line directly into the existing tanks does not work with gravity flow, a pump could be installed to pump water from the new tanks to the existing tanks. This pump could run on the green energy grid, and could be turned on to replenish water in the current tanks when there is an excess of green energy available. This option would require a gutter system to be installed on the Pole Barn roof, increasing water collection capabilities as well as the amount of water storage.

Additionally, Option 2, putting tanks up a hill near the garden, seems impractical. A water tower or tank elevation of 19 feet would be required for successful gravity feeding to the drip irrigation system, and the materials and machines required for this project would be costly to the island. A tower of this height would cause accessibility issues for both general maintenance and winter months, when the system is drained and taken down. This would also pose aesthetic issues considering its proximity to the Celia Thaxter garden, where garden tours are conducted. Multiple tanks would be difficult and extremely costly to install, and overall the timely installation process would not be worth the time required for completion.

5.7 References

"Precipitation." *Sustainable SML*, Shoals Marine Laboratory, https://sustainablesml.org/pages/detail.php?tile=tower_wunderground_daily.

Future Project Suggestions

Rainwater Collection

Future interns could look at the logistics of attaching the garden hose to rainwater collection tanks, so water from the hose does not deplete well water stores.

Power Of Wind

Devise a method to install an anemometer on top of the turbine or closer to the turbine in location and height and expand the analysis with more accurate wind speed values to gain a better understanding of the effectiveness of the wind turbine. Having another year of AcuDC vs VSCII data will help determine a more accurate power offset to use.

Expanded Life Cycle Analysis

LCA is an extremely useful tool for holistically evaluating the sustainability initiatives at Shoals. Additional systems such as the electrical and wastewater could be analyzed to help further quantify the effectiveness of Shoal's sustainability.

Building Electricity Use Analysis

Calculate the energy use for each building on the island to understand how the electricity resources are distributed. Suggest methods to reduce high-electricity use buildings.

Appendix A Topographic Map of Appledore Island

Appendix B All Normalized Wind Speed Histograms

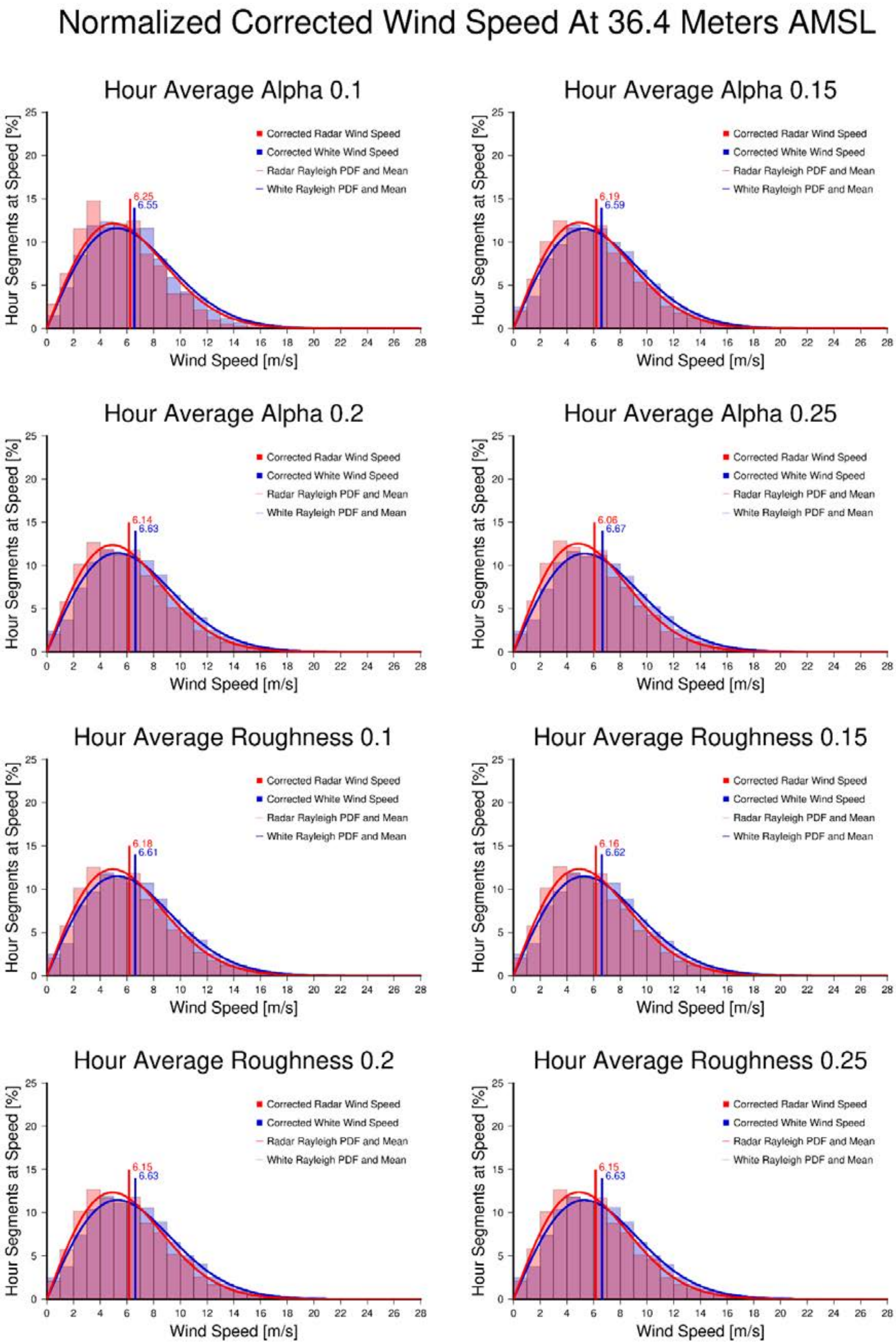

Appendix C SimaPro Inputs for Manufacturing Phase

Component	Material	Explanation	Value	SimaPro Input
Reverse Osmosis	Fiberglass	Green Tank	34.56 kg	Glass fibre reinforced plastic, polyamide, injection moulded {GLO}| market for | APOS, U
	Pump	Ocean to Reverse Osmosis	1 pump	Water pump, 22kW {GLO}| water pump production, 22kW | APOS, U
	Pump	Reverse Osmosis to Cistern	1 pump	Water pump, 22kW {GLO}| water pump production, 22kW | APOS, U
	Polyethylene	Plastic Pipes	4 kg	Polyethylene pipe, DN 200, SDR 41 {GLO}| market for polyethylene pipe, DN 200, SDR 41 | APOS, U
	Steel	Machine Body	410 kg	Steel, low-alloyed {GLO}| market for | APOS, U
Well	Concrete	Octagon Base of Well	100 ft^3	Concrete, medium strength {RoW}| market for concrete, medium strength | APOS, U
	Tin	Well Sides	4300 kg	Tin {GLO}| market for | APOS, U
	Polypropylene	Corrigated Plastic Well Roof	113.3 ft^2	Polypropylene, granulate {GLO}| market for | APOS, U
	Wood	Well Roof	16.49 ft^3	Lumber, softwood, ACQ treated, SE/m3/RNA
	Pump	Well to Cistern	1 pump	Water pump, 22kW {GLO}| water pump production, 22kW | APOS, U
	PVC	Pipe	52 kg	Polyvinylchloride, suspension polymerised {GLO}| market for | APOS, U
	Polyethylene	Plastic Pipes Well to Cistern	36 kg	Polyethylene pipe, DN 200, SDR 41 {GLO}| market for polyethylene pipe, DN 200, SDR 41 | APOS, U
Cistern	Pump	Cistern To Pressure Tank	1 pump	Water pump, 22kW {GLO}| water pump production, 22kW | APOS, U
	Polyethylene	Plastic Pipes Well to Cistern	4 kg	Polyethylene pipe, DN 200, SDR 41 {GLO}| market for polyethylene pipe, DN 200, SDR 41 | APOS, U
	Brick	Lines Tank	10280 kg	Clay brick {GLO}| market for | APOS, U
	Concrete	Lines Tank	143 ft^3	Concrete, medium strength {RoW}| market for concrete, medium strength | APOS, U
	Pump	Chlorine Pump	2 pumps	Water pump, 22kW {GLO}| water pump production, 22kW | APOS, U
	PVC	Pipe	52 kg	Polyvinylchloride, suspension polymerised {GLO}| market for | APOS, U
	Polyethylene	Chlorine Tubing	0.03 kg	Polyethylene pipe, DN 200, SDR 41 {GLO}| market for polyethylene pipe, DN 200, SDR 41 | APOS, U
Pressure Tank	Stainless Steel	Tank	8512 kg	Steel, chromium steel 18/8, hot rolled {GLO}| market for | APOS, U
	Polyethylene	Plastic Pipes	44 kg	Polyethylene pipe, DN 200, SDR 41 {GLO}| market for polyethylene pipe, DN 200, SDR 41 | APOS, U
Distribution System	Polyethylene	Plastic Pipes	370 kg	Polyethylene pipe, DN 200, SDR 41 {GLO}| market for polyethylene pipe, DN 200, SDR 41 | APOS, U
	Copper	Junction Valves	5 kg	Copper {RoW}| production, primary | APOS, U
Transportation	Lorry	Reverse Osmosis to Portsmouth	2005886 kg km	Transport, freight, lorry, unspecified {RoW}| market for transport, freight, lorry, unspecified | APOS, U
	Diesel	Portsmouth to Appledore	400 gal	Diesel {GLO}| market group for | APOS, U
Packaging	Cardboard	Packaging	23 kg	Corrugated board box {RoW}| market for corrugated board box | APOS, U
	Polyethylene	Plastic - Bubble Wrap Packaging	9 kg	Polyethylene, linear low density, granulate {GLO}| market for | APOS, U

Appendix D Erosion Control Site Visit Tables

SITE VISIT INFORMATION FOR EROSION CONTROL TREATMENT SELECTION	
Name	Tess Hays & Izzy Medeiros
Location	Coastal slope along western side of island
Weather	windy, clouds
Date	6/16/22
Project	Erosion Control - Site 1
SOIL	
Moisture Conditions of Soil	dry, powdery, dusty
Depth	shallow
Rock Coverage	minimal immobile rocks, moderately large gravel, small gravel (grape sized) and fines
Soil Type	LyB
VEGETATION	
Vegetation Description	sparse cover on mid road, edges of road have small shrubs, weeds, smal trees, heavier on inland side, but thick both sides
TOPOGRAPHY	
Slope Angle	6.0°
Slope Length	208 feet
Slope Aspect	from south to north
EROSION PROCESSES	
Water Erosion	severe at cut out, moderate on the road
GENERAL COMMENTS:	large rocks inland side would make it hard to build a swale, diverted runoff would be moved if road was adjusted, potential water flow from two sources/paths (convergence at peak of hill)

SITE VISIT INFORMATION FOR EROSION CONTROL TREATMENT SELECTION	
Name	Tess Hays & Izzy Medeiros
Location	S-turn and the road east of the radar tower
Weather	windy, clouds
Date	6/16/22
Project	Erosion Control - Site 2
SOIL	
Moisture Conditions of Soil	dry patches, moist on swale side
Depth	shallow
Rock Coverage	bigger rocks where there is erosion, more fines near the swale, large rock cover upside
Soil Type	LyB & LyC
VEGETATION	
Vegetation Description	more grass in the road than S1, edges still tall frass, thicker veg than S1 on both sides
TOPOGRAPHY	
Slope Angle	4.7°
Slope Length	230 feet
Slope Aspect	southeast to northwest
EROSION PROCESSES	
Water Erosion	more severe up hill where there's no natural swale off-road
GENERAL COMMENTS:	sideways on higher elevation, potential runoff system at high point in path

SITE VISIT INFORMATION FOR EROSION CONTROL TREATMENT SELECTION	
Name	Tess Hays & Izzy Medeiros
Location	Same location as Site 2, perpendicular to Site 2
Weather	Cloudy
Date	7/1/22
Project	Erosion Control - Site 2B
SOIL	
Moisture Conditions of Soil	dry, powdery, dusty
Depth	shallow
Rock Coverage	consistently more fine than other sites
Soil Type	LyC
VEGETATION	
Vegetation Description	encroaching on the road, thicker on the northern side, more bushy on the southern side
TOPOGRAPHY	
Slope Angle	4.9°
Slope Length	81 feet
Slope Aspect	west to east
EROSION PROCESSES	
Water Erosion	rutting
GENERAL COMMENTS:	fil was recently placed

SITE VISIT INFORMATION FOR EROSION CONTROL TREATMENT SELECTION	
Name	Tess Hays & Izzy Medeiros
Location	Road from Kingsbury to Leighton, to the west of the radar tower
Weather	windy, clouds
Date	6/16/22
Project	Erosion Control - Site 3
SOIL	
Moisture Conditions of Soil	dry and powdery
Depth	very shallow, ledge at surface
Rock Coverage	visual ledge partially covered, coarse gravel varying sizes
Soil Type	LyB & LyC
VEGETATION	
Vegetation Description	more grass in center, shrubs and grass line roadway
TOPOGRAPHY	
Slope Angle	5.1°
Slope Length	345 feet
Slope Aspect	east to southwest
EROSION PROCESSES	
Water Erosion	natrual swale in road, water cannot drain
GENERAL COMMENTS:	lots of ledge for potential natural level spreader

SITE VISIT INFORMATION FOR EROSION CONTROL TREATMENT SELECTION	
Name	Tess Hays & Izzy Medeiros
Location	Coastal slope along western side of island, continuing past the dock
Weather	Cloudy
Date	7/1/22
Project	Erosion Control - Site 4
SOIL	
Moisture Conditions of Soil	dry, powdery, dusty
Depth	shallow
Rock Coverage	fines at the top, more gravel lower
Soil Type	LyB & LyC
VEGETATION	
Vegetation Description	grass on northern side, much more dense on southern side
TOPOGRAPHY	
Slope Angle	1.7° - 3.2°
Slope Length	378 feet
Slope Aspect	northeast to southwest; southwest to northeast
EROSION PROCESSES	
Water Erosion	minimal, more severe towards Site 1
GENERAL COMMENTS:	geotextiles may need to be removed or replaced